

DEPOSIT CONSTITUENT PHASE SEPARATION AND ADHESION

E. RAASK

Technology Planning and Research Division, Central Electricity Generating Board,
Kelvin Avenue, Leatherhead, Surrey, UK

The initial deposit material on coal fired boiler tubes consist largely of silicate, sulphate and iron oxide particles. The fused silicates and molten sulphates form immiscible phases at high temperatures first on the micro-scale in individual particles and subsequently as separate layers in the deposit. The adhesion of ash deposit constituents to boiler tubes starts with the small particle retention as a result of the van der Waals, electrostatic and liquid film surface tension forces. Subsequently a strong bond will develop between the oxidized metal surface and iron saturated layer of ash deposit.

The pulverized coal fired boilers at electricity utility power stations are designed for "dry" ash operation where the bulk of mineral matter residue is removed in the electrical precipitators in the form of particulate ash. However, it is inevitable that some deposits of sintered ash and semi-fused slag form on the heat exchange tubes and between 20 and 30 per cent of coal ash is discharged from the combustion chamber as clinker. The high temperature cyclone fired boilers are designed for "wet" ash operation and up to 80 per cent of coal ash is discharged from the furnace as molten slag.

The build-up of sintered ash and fused slag deposits depends chiefly on the rate of ash particle impaction and the adhesive characteristics of the collecting surface. The initial deposit on the heat exchange tubes in pulverized coal fired boilers consists of ash particles of diameter ranging from less than 0.1 μm to 100 μm . Subsequently the deposited ash may be re-entrained in the flue gas or it may form first a sintered matrix and later a fused slag deposit chiefly by viscous flow. For the deposit formation the ash particles must be first held at the collecting surface and subsequently the deposit matrix bonded to the boiler tubes by adhesive forces sufficiently strong to overcome the gravitational pull, boiler vibration and eventually the sootblower jet impaction. This work sets out to examine the adhesive characteristics of different constituents of the flame heated ash and the formation of sintered deposits and slag bonded to the heat exchange tubes.

INITIAL DEPOSIT CONSTITUENTS

The mineral matter in coal consists chiefly of silicate, sulphide, carbonate species, and chlorides and organo-metal compounds associated with the fuel substance (1,2). The silicate mineral particles vitrify partially or completely, in the pulverized coal flame (3), and thus the silicate ash fraction of the initial deposit consists of particles of variable amounts of a glassy phase and crystalline species (4).

The sulphide, carbonate, chloride and organo-metal species dissociate and oxidize in the flame. The oxides may remain as discrete particles, chiefly iron oxide (magnetite), can dissolve in the glassy phase of silicates, and a fraction of calcium and sodium oxides are sulphated (5). Thus the initial deposit material will contain some calcium, sodium and potassium sulphate. The latter originates from the release of potassium in the flame heated aluminosilicate particles (6).

The relative concentrations of flame heated ash constituents, namely silicates, iron oxide and sulphate can be estimated from the ash analysis. However, the composition of the initial deposit material can be markedly different as a result of selective deposition. In particular, the deposit material can be enriched in sulphate as shown in Fig. 1. The relative concentrations of different deposit constituents were obtained by analysing the material on a cooled metal tube probe inserted in boiler flue gas for short, 2 to 15 minute duration (7). The sulphate content of the flue gas borne ash and probe deposits in a cyclone fired boiler was higher than that in the pulverized coal fired boiler ash and deposits. This was because in cyclone boilers the bulk of silicate ash is discharged as molten slag but the residual ash is relatively rich in sulphate.

The rate of alkali-metal sulphate deposition will decrease when the temperature of collecting target surface exceeds 1075 K as shown in Fig. 2. The decrease in the deposition of alkali-metal sulphates is related to the concentration of the volatile alkali-metals in the flue gas and the saturation vapour pressure of sodium and potassium sulphates (8). The initial deposit on cooled surfaces contains a small amount of chloride as shown in Fig. 2.

In a reducing atmosphere the deposit material may contain iron sulphide (FeS) formed on dissociation of coal pyrite mineral. This is likely to occur on the combustion chamber wall tubes near the burners where the reaction time is short, below one second, for oxidation of FeS residue to the oxide. It has been suggested that calcium sulphide (CaS) may also be present in the ash material deposited from a reducing atmosphere gas stream as a result of sulphidation of calcium oxide (9).

THERMAL STABILITY OF SULPHATES AND IMMISCIBILITY WITH SILICATES

Bituminous coals usually leave a highly silicious ash on combustion. That is, fused aluminosilicates constitute an acidic media at high temperatures that is capable of absorbing large quantities of basic metals in the form of oxides, chiefly those of sodium, calcium and magnesium. At lower temperatures the corresponding sulphates are thermodynamically more stable in the presence of sulphur gases. The equilibrium distribution of alkaline oxides between molten sulphates and fused silicates at different temperatures can be calculated from the appropriate thermodynamic data. However, the residence time of the flame borne mineral species before deposition is short and the alkali-metal distribution does not reach the equilibrium state.

The fused silicate particles will absorb the flame volatilized sodium to the depth of about 0.05 μm (10), and the remainder is converted to sulphate partly in the flue gas and partly at the surface of ash particles. The distribution of sodium in the silicate and sulphate phases can be expressed in a form:

$$m_{\text{sul}} = m_0 - kw^{2/3} \quad \dots 1)$$

$$\text{where } m_{\text{sil}} + m_{\text{sul}} = m_0 \quad \dots 2)$$

m_{sil} , m_{sul} and m_0 denote the amount of sodium in silicate and sulphate fractions, and the total sodium in ash respectively; k is a constant and w is the ash content of coal. When the sodium to ash ratio is below 1 to 100 the bulk of sodium is captured by the silicate particles and equation 2 reduces to:

$$m_{sil} \approx m_o$$

... 3)

and consequently the amount of sodium available for the formation of sulphate is small.

The molten sodium sulphate/sodium silicate system of composition Na_2SO_4/Na_2O-SiO_2 has one liquid phase at 1475 K, but as the proportion of silica increases, the melt separates into two layers (11,12). The change from the miscible to immiscible phase of the system has been explained by alterations in the silicate structure as the ratio of Na_2O to SiO_2 decreases. In more basic, less viscous melts, the silicate ions exist in the form of SiO_4^{4-} tetrahedrons which have the same mobility as sulphate ions, and thus homogeneity of the system is to be expected. As the silica content is increased the complexity of the silicate structure reaches a point where the silica anions become relatively immobile for a separation of sulphate from silica to take place.

The miscibility of the corresponding potassium sulphate-silicate system has been studied by the usual crucible method as well as by a technique of a hanging droplet (13). The droplets of potassium sulphate/silicate mixtures, 3 mm in diameter, were suspended from 0.5 mm platinum wire which had a semi-spherical head 1.5 mm in diameter. Separation of the silicate (internal) and sulphate phases in the droplets can be observed directly in the Leitz heating microscope which is used, in its conventional mode of operation, to assess the fusion characteristics of coal ashes (14). Fig. 3 shows the two phase separation of $2K_2SO_4-K_2O-2SiO_2$ system at 1575 K where the outside envelope is the transparent sulphate phase through which the platinum wire heats (top) and a globule of molten silicate (bottom) can be seen. As the temperature was increased to 1725 K the two phases became miscible because of the increased solubility of sulphate in the silicate melt at the higher temperature.

The $K_2SO_4-K_2O-SiO_2$ phase diagram is depicted in Fig. 4 which shows that the system is miscible at 1575 K when the molar ratio of K_2O to SiO_2 is above 0.5. As in the corresponding sodium sulphate/sodium silicate system, less basic melts separate into two immiscible liquids. This is the case with most coal ash slags where the molar ratio of basic oxides (sum of Na_2O , K_2O , CaO and MgO) to SiO_2 is well below 0.5. Exceptions to this are the sodium and calcium rich ashes of some lignite and non-bituminous coals, which can have sufficient amounts of alkalis to form a single phase melt of miscible sulphates and silicates at high temperatures.

ADHESION BY VAN DER WAALS AND ELECTROSTATIC FORCES

The ash particles deposited on boiler tubes are initially held in place by surface forces, i.e. van der Waals and electrostatic attraction forces. Van der Waals forces become important when molecules or solid surfaces are brought close together without a chemical interaction taking place. For a hemispherical particle of radius (r) held at a distance of nearest approach (h) from a plane, the resultant forces (F) is given by:

$$F = \frac{Ar}{6h^2} \quad \dots 4)$$

where A is the Hamaker constant (15).

Equation 4 applies over short distances, up to 150 Å (1.5×10^{-8} m) and for longer distances the "retarded" van der Waals forces decay rapidly (16). An equation based on the dielectric properties of solids for the retarded

van der Waals forces (F') between a sphere of radius (r) at the distance (h) from a flat surface is (17):

$$F' = \frac{2B\pi r}{3h^3} \quad \dots 5)$$

where B is the appropriate constant for the given material.

The changeover from the unretarded to retarded van der Waals forces occurs at a distance of about 150 \AA ($1.5 \times 10^{-8} \text{ m}$), and the corresponding value of the Hamaker constant (A) in equation 4 was found to be 10^{-19} N (Newton), and that of the Lifshitz constant (B) in equation 5 was $8.9 \times 10^{-29} \text{ N m}$ (16,18). These values have been used to compute the ratio of van der Waals forces to the gravitational force on small ash particles approaching a flat surface.

The gravitational force (F_g) on an ash particle of radius (r) and the density (D) is given by:

$$F_g = \frac{4\pi r^3 Dg}{3} \quad \dots 6)$$

where g is the gravity acceleration constant (9.81 m s^{-2}). Thus, the ratio (F_r) of the short distance van der Waals forces (F) to the gravitational force (F_g) on a particle is:

$$\frac{F}{F_g} = F_r = \frac{A}{8\pi Dgr^2 h^2} = \frac{1.62 \times 10^{-25}}{r^2 h^2} \quad \dots 7)$$

where the value of D for ash was taken to be 2500 kg m^{-3} and when $h < 1.5 \times 10^{-8} \text{ m}$. The corresponding ratio (F_r') of the retarded van der Waals forces (F') to the gravitational force is given by:

$$\frac{F'}{F_g} = F_r' = \frac{2B}{Dgr^2 h^3} = \frac{8.15 \times 10^{-34}}{r^2 h^3} \quad \dots 8)$$

where $h > 1.5 \times 10^{-8} \text{ m}$.

Fig. 5 shows a comparison of van der Waals and the gravitational forces on small ash particles as these approach a collecting surface. Plots A and B indicate that the sub-micron sized particles are readily held on a surface by van der Waals forces. The capture of small particles of ash on boiler tubes is further enhanced by surface irregularities of oxidized metal (19). Also, it has been suggested that an electrostatic attraction force enhance the transport and retention of sub-micron sized particles on steel probes inserted in the flue gas of coal fired boilers (7,20). A layer of electrically precipitated deposit of ash can have a cohesive strength between 5 and 40 times higher than that formed by sedimentation because particles in an electric field have permanent dipole characteristics which lead to these being orientated to form a cohesive layer of ash (21). It appears therefore that the combined effects of van der Waals and electrostatic forces of attraction, and surface irregularities are sufficient to hold the sub-micron diameter particles on the surface of boiler tubes for the subsequent liquid phase adhesion, and chemical and mechanical bond formation.

ADHESION BY SURFACE TENSION FORCE

The formation of strong adhesive bonds of enamel coatings and glass/metal seals on heating requires the presence of a liquid phase (22,23,24). The role of the liquid film is to provide the initial adhesion of solid particles as a result of surface tension. The work of adhesion (W_a) is given by:

$$W_a = \pi + \gamma (1 + \cos \theta) \quad \dots 9)$$

where γ is the surface tension of the liquid, and θ is the contact angle at the solid/liquid interface. With perfect wetting, i.e. when θ equals zero, W_a has the highest value:

$$W_a = \pi + 2\gamma \quad \dots 10)$$

The work of cohesion of a liquid (W_c) is given by:

$$W_c = 2\gamma \quad \dots 11)$$

With wetting liquids, therefore, W_a can be higher than W_c and failure will take place within the liquid layer, whereas with non-wetting liquids the rupture occurs at the solid/liquid interface.

Alkali-metal sulphates frequently constitute a liquid phase in ash deposits, and the molten sulphates readily wet and spread on the surface of boiler tubes. In a reducing atmosphere and when in contact with carbon, sulphates are reduced to sulphides which wet and spread on any surface. The coefficient of surface tension of sulphates is fairly high, 0.20 N m^{-1} for Na_2SO_4 and 0.14 N m^{-1} for K_2SO_4 near their respective melting point temperatures (25,26). Thus work of cohesion of molten sulphate layer in boiler deposit is between 0.3 and 0.4 N m^{-1} and the work of adhesion is higher because of a low contact angle at the sulphate/tube surface interface. It is therefore to be expected and it is observed in practice that when the deposit is removed, e.g. by sootblowing, there remains a film of sulphate adhering to boiler tubes. The surface tension of coal ash slag has been measured previously by the sessile drop method (27) and a typical value was 0.3 N m^{-1} . It is about twice that of sulphates and thus the work of adhesion (Equation 9) and the cohesive bond strength are corresponding higher at the slag/solid interface.

Only a small amount of liquid, about a hundred molecule thick layer, is sufficient for the adhesion contact of sub-micron diameter particles (28). In the case of a volatile liquid, the equilibrium thickness of the film, and thus the adhesion, varies with partial pressure of the vapour in the surrounding atmosphere. When evaporation from a liquid film occurs, as a result of increased temperature, the adhesion first rises to a maximum value due to the meniscus effect but it breaks down as the film thickness is reduced to molecular dimensions. However, before the break-down of the surface tension chemical and mechanical bonds may develop between the deposited ash and boiler tube surface.

MECHANICAL AND CHEMICAL BONDING

Ash deposits on boiler tubes can be keyed to the surface of metal oxide by mechanical and chemical bonds. Mechanical bonding is enhanced by extending surface at the interface as shown in Fig. 6a. Boiler tubes are not polished and thus have an extended surface that is further increased by oxidation and chemical reactions between the oxide layer and ash deposits. It is therefore evident that a comparatively rough surface of boiler tubes constitute an anchorage for keying ash deposits to the heat exchange elements.

Dietzel (29) and Staley (30) have proposed that the chemical reactions at a enamel/metal interface can be considered in terms of electrolytic cells set up between the metals of different electro-chemical potential. It has been suggested that cobalt or nickel precipitated in the enamel when in contact with steel surface, forms short-circuited local cells in which iron is the anode. The current flows from iron through the melt to cobalt and back to iron. The result is that iron goes into solution, the surface becomes roughened, and the enamel material anchors itself into the cavities as shown in Fig. 6b.

The galvanic reactions will take place at a much faster rate in the low viscosity phase of sulphates in boiler deposit than that in highly viscous silicate glass. However, rapid reactions at the tube surface/deposit interface may not be necessary or appropriate for development of a strong bond between the ash deposit and boiler tubes. In metal/glass seal and metal/enamel coating technology, the adhesive bonds formed on heating have to be completed in a few hours, whereas those in boiler deposits can form over a period of days or weeks. The adhesive bond between the metal surface and a silicate material can be high when there is a gradual rather than abrupt change in the glass phase composition near the interface (31).

When the ash deposit is brought in intimate contact with the surface of boiler tubes either by the action of surface tension or by the galvanic reactions, the controlling parameter in mechanical bonding is the strength of the glassy phase at the narrowest cross sectional area of contact cavities (Fig. 6b). The annealed glass may have a tensile strength of around 50 MN m^{-2} giving a maximum bond strength of 35 MN m^{-2} . However, the glass at the interface may be stronger or weaker depending on whether the conditions in the keying cavities increase or decrease local flaws and resultant stresses.

Chemical bonds, covalent or ionic as shown in Fig. 6c and d, at the metal oxide/deposit surface are potentially strong with theoretical values over 10^9 N m^{-2} . It is, however, impossible to estimate the number of sites and the size of contact areas at the interface where the chemical bonds may be effective. In any case, the cohesive strength of the deposit matrix is the limiting factor since it is lower than that of chemical bonds by several orders of magnitude. In practice, this means that when a strongly adhering deposit is subjected to a destructive force, e.g. sootblower jet, failure occurs within the deposit matrix and there remains a residual layer of ash material firmly bonded to the tube surface.

ADHESION OF ASH DEPOSITS ON FERRITIC AND AUSTENITIC STEELS

The adhesion bond strength of soda glass on a metal substrate has been determined by heating a glass disc sandwiched between two metal discs in a vertical furnace (32). The technique has been adopted for measuring the strength of the adhesive bond developed when a boiler deposit was sandwiched between two discs of ferritic or austenitic steels (33). The deposit material was taken immediately after boiler shut-down from the superheater tubes of a pulverized coal fired boiler fuelled with a mixture of East Midlands, UK coals. The flue gas temperature in the superheater prior to boiler shut-down was about 1300 K and the tube metal temperature was 850 K. The deposit material consisted of 30 per cent of alkali-metal sulphates in weight ratio of 2 to 1 of Na_2SO_4 to K_2SO_4 , the remainder being silicate ash. A layer of deposit, 3 mm thick, was sandwiched between two metal discs, 20 mm in diameter, made of boiler tube steels and then heated in a vertical furnace. After a time interval lasting from one to 25 days the bond was ruptured by applying a tensile force without prior cooling.

The results in Fig. 7 show that the strength of adhesive bond between the ferritic steel sample and boiler deposit increased exponentially with

temperature in the range of 775 to 900 K. Similar results were obtained by Moza et al. (34) who used a droplet technique to measure the adhesive bond of coal ash slag on a ferritic steel target in the temperature range of 700 to 950 K.

The results plotted in Fig. 8 shows that the strength of adhesive bond of ash deposit on both the ferritic and austenitic steels increased approximately linearly with time at 900 K. However, the bond strength of deposit on the austenitic steel (Type 18Cr13NiNb) was significantly lower than that between the deposit and 9Cr-ferritic steel. The latter resulted from the thermal and chemical compatibility of the steel oxide layer and deposit material (35). Table 1 shows approximate values of the coefficient of thermal expansion of the ferritic and austenitic steels, some oxides and silicate materials (36).

Table 1: Coefficient of Thermal Expansion of Boiler Tube Steels, Oxides and Silicates

Material	Thermal Expansion, $\frac{\Delta m}{m} K^{-1}$
<u>Steels</u>	
Mild Steel and Ferritic Steels	11 to 12 $\times 10^{-6}$
Austenitic Steels	16 to 18 $\times 10^{-6}$
<u>Oxides</u>	
Tube Metal Oxides (Fe ₃ O ₄ , Cr ₂ O ₃ , NiO)	8 to 10 $\times 10^{-6}$
<u>Deposit Constituents</u>	
Glassy Material	6 to 9 $\times 10^{-6}$
Quartz (Crystalline)	5 to 8 $\times 10^{-6}$
Silicates in Fired Brick	7 to 8 $\times 10^{-6}$

The data in Table 1 show that the coefficient of thermal expansion of mild steel and ferritic steels is not greatly different from that of their oxides and the ash deposit constituents. It is therefore evident that there is no gross incompatibility in the thermal expansion characteristics and strongly bonded ash deposits once formed on mild steel tubes are not easily dislodged on thermal cycling.

In contrast, the thermal expansion of austenitic steel is significantly higher than that of the oxides and deposit material. In the absence of boiler deposit, the oxide material in the form of thin layer is able to absorb thermal stresses and the adhesive layer remains intact on cooling. However, it appears that the oxide layer is unable to absorb thermal stresses in a similar manner when contaminated and constrained by bonded ash deposits. It is therefore a usual occurrence that ash deposits peel off the austenitic steel tubes on cooling whereas the deposit formed on ferritic steels under the same conditions remain firmly attached to the tubes.

King et al. (22) have suggested that in order to obtain good adherence of enamel coatings on metals, the enamel material at the interface must become saturated with the metal oxide, e.g. FeO of ferritic steels. Coal ash deposit on boiler tubes contains between 5 and 25 per cent iron oxide (Fig. 1) and thus the layer at the tube/deposit interface becomes saturated with FeO. The chromium and nickel contents of ash deposit are low and thus the same chemical compatibility stage is not reached at the austenitic steel/deposit interface.

The adhesive bond between boiler ash deposit and the surface of ferritic steels can attain exceptionally high strengths. This was found on examining the deposits formed on different steel specimens tested in an experimental superheater loop. Favourable conditions for the formation of firmly bonded deposits were as follows:

- (a) The iron oxide content of coal was above 20 per cent expressed as Fe_2O_3 giving an iron saturated layer of deposit on the tube specimens.
- (b) The ash collecting surface was a 5 per cent chromium ferritic steel which formed an oxide layer strongly adhering to metal for a firm anchorage of deposits.
- (c) The tube metal temperature was high, 950 K, which enhanced the formation of strong adhesive bond. The flue gas temperature at that position was approximately 1250 K.
- (d) The ferritic test piece in the experimental loop was sheltered from direct action of sootblower. Weak turbulence caused by the jet removed some of the unsintered silica ash leaving iron rich deposit firmly bonded to the tube. The iron rich deposit had grown in thickness to about 20 mm after nine months, and cohesive strength of the deposit material increased towards the surface of tube metal. The microscopic examination showed that there was no marked interface boundary between the ash deposit and metal oxide.

FORMATION OF LAYER STRUCTURE DEPOSITS AND SLAG MASSES

The coal ash deposits on boiler tubes have frequently a separate zone structure with a sulphate rich layer up to 2 mm thick under the matrix of sintered ash (35). The outer layer is porous and it constitutes a pathway for the enrichment of alkali-metals in the deposit layer next to tube surface. The diffusible species may be sulphate, chloride, oxide or hydroxide, but the thermodynamic data (8) and the results of deposition measurements in coal fired boilers (Fig. 3) suggest that sodium and potassium sulphates are the principal vapour species which diffuse through a porous matrix of silicate ash deposit.

The relative amounts of Na_2SO_4 and K_2SO_4 which diffuse through the sintered matrix of silicate ash depend on the temperature gradient across the deposit layer, vapour pressure of the species and thermodynamic stability of the sulphates in the presence of silicates. Potassium sulphate has a higher temperature stability limit when compared with that of sodium sulphate and as a result K_2SO_4 can be preferentially transported to the surface of cooled boiler tubes when there is a steep temperature gradient across the ash deposit. The K_2SO_4 rich phase, when molten, can cause severe corrosion of tube metal.

The corrosion product, a mixture of oxide, sulphide at the metal interface and sulphate outside, has a weak adhesive bond to the metal surface and cannot support large deposit masses. It is therefore unusual to find excessive amounts of sintered ash deposits and fused slag in the exact localities where severe high temperature corrosion occurs. Conversely, a strongly adhering matrix

of sintered ash deposit in the absence of sulphate, sulphide or chloride phases is not markedly corrosive.

The build-up of boiler tube deposits is a continuously changing process as depicted in Fig. 9. When the deposit material reaches a thickness of 2 to 3 mm (Fig. 9a) the separate sulphate and silicate phases occur (Fig. 9b). Subsequently, the sulphate layer disappears in the middle section (Fig. 9c) allowing a strong bond to be established between the sintered ash deposit and ferritic steel boiler tubes. This is the "classical" mode of formation of superheater tube deposit when the metal temperature is in the range of 750 to 900 K. Above 950 K the layer structured deposits are less likely to occur and a strong adhesive bond is rapidly formed between the silicate ash deposits and the high temperature tube surface.

A notable feature of slag formed in pulverized coal fired boiler is its variable gas hole porosity. Burning coal particles are encapsulated in the deposit layer and generate CO and CO₂ inside the silicate material (27) resulting in a highly porous slag. The density of slag will increase when the encapsulated coal particles are consumed and gas bubbles have escaped.

It has been observed that new boilers have an "immunity" period lasting weeks or months before severe slag build-up occurs. This is partly due to the fact that during the commissioning period the boiler rarely reaches full load output. However, it may also be partly due to a slow rate of formation of the interface layer on boiler tubes which is able to have a strong adhesive bond to rapidly forming ash slag and thus able to support large masses of deposit.

CONCLUSIONS

Initial Deposit

The initial deposit material on cooled tubes in coal fired boilers consists largely of flame vitrified silicate ash, iron oxide, and calcium and alkali-metal sulphates. Trace amounts of chloride will also deposit and under reducing conditions some iron and calcium sulphides can be present.

Phase Separation

Most coals leave an ash residue which is pyrochemically acidic, and the alkali-metals and calcium are distributed in the silicate and sulphate phases under oxidizing conditions. The fused silicates and molten sulphates are immiscible and separate into two phases. The phase separation enhances the adhesion of ash to boiler tubes and leads to the formation of layer structured deposits.

Initial Particle Adhesion

Initially the small particles of ash, below 1 μm in diameter are held at the surface of boiler tubes by the van der Waals and electrostatic attraction forces. Subsequently a film of molten sulphate may form at the tube surface/deposit interface and only a small amount of liquid, about one hundred molecules thick is sufficient for bonding.

Strong Adhesive Bond of Deposits on Ferritic Steels

Strong adhesive bonds can form between the oxidized surface of ferritic steels and iron rich ash because of the composition and thermal expansion compatibility of the metal oxide and silicate ash deposit. The adhesive bond strength increases exponentially with temperature of the target surface in the

range of 750 to 950 K. The bond strength can reach high values, that is, higher than the cohesive strength of sintered ash deposits at temperatures above 850 K.

Weak Adhesive Bond of Deposits on Austenitic Steels

The adhesive bond between the austenitic steel surface and ash deposit is relatively weak as a result of the composition and thermal incompatibility of the steel oxide and the silicate material. The temperature fluctuations on changeable boiler load conditions can cause sufficiently high thermal stresses for deposit to skid off the austenitic steel tubes.

Boiler Tube/Ash Deposit Interface

The boiler tube/ash deposit interface layer which can support large masses of slag formed in the combustion chamber takes several months to develop. Thus the full extent of boiler slagging may not become evident during the commissioning period of new boiler plant.

ACKNOWLEDGEMENT

The work was carried out at the Central Electricity Research Laboratories and the paper is published by permission of the Central Electricity Generating Board.

LITERATURE CITED

1. Lowry, H.H., Editor, "Chemistry of Coal Utilization", John Wiley and Sons, Inc., New York, (1963)
2. Francis, W., "Fuels and Fuel Technology", Vol. I, Pergamon Press, London, (1965)
3. Raask, E., "Fusion of Silicate Particles in Coal Flames", Fuel, (1969), 48, 366
4. Raask, E. and Goetz, L., "Characterization of Captured Ash, Chimney Stack Solids and Trace Elements", Jour. Inst. Energy, (1981), 54, 163
5. Raask, E., "Sulphate Capture in Ash and Boiler Deposits in Relation to SO₂ Emission", Proc. Ener. Comb. Sci., (1982), 8, 261
6. Raask, E., "The Behaviour of Potassium Silicates in Pulverized Coal Firing", VGB Mitteilungen, (1968), 18, 348
7. Raask, E., "Reactions of Coal Impurities during Combustion and Deposition of Ash Constituents on Cooled Surfaces", Conf., Mechanism of Corrosion by Fuel Impurities, p. 145, Marchwood, UK, Butterworth Publ., London, (1963)
9. Halstead, W.D. and Raask, E., "The Behaviour of Sulphur and Chlorine Compounds in Pulverized Coal Fired Boilers", Jour. Inst. Fuel, (1969), 43, 344
9. Hein, K., "Chemical and Mineralogical Aspects of Fouling of Heat Exchange Surfaces in Non-Bituminous Coal Fired Boilers", VGB Kraftwerkstechnik, (1979), 59, 576
10. Hosegood, E.A. and Raask, E., "Reactions and Properties of Alkalis and Ash in Pulverized Fuel Combustion", CERL Note No. RD/L/N 49/64, Leatherhead, UK, (1964)

11. Kordes, E., Zofelt, B. and Proger, H.J., "Reactions in the Melting of Glass with Na_2SO_4 : Immiscibility Gap in Liquid State between Na-Ca-Silicates and Na_2SO_4 ", *Zeitschr. Anorg. Allgem. Chem.*, (1951), 264, 255
12. Pearce, M.L. and Beisler, J.F., "Miscibility Gap in the System Sodium Oxide-Silica-Sodium Sulphate at 1473 K", *Jour. Am. Cer. Soc.*, (1965), 48, 40
13. Raask, E. and Jessop, R., "Miscibility Gap in the Potassium Sulphate-Potassium Silicate System at 1575 K", *Phys. and Chem. Glasses*, (1966), 7, 200
14. DIN, "Determination of Ash Fusion Behaviour", German Standard, DIN 51 730, (1976)
15. Casimir, H.B.G. and Polder, D., "The Influence of Retardation on the London-van der Waals Forces", *Phys. Rev.*, (1948), 73, 360
16. Tabor, D., "Surface Forces", *Chem. Ind.*, (1971), No. 35, p 969
17. Lifshitz, E.M., "The Theory of Molecular Attractive Forces Between Solids", *Soviet Physics, JETP*, (1956), 2, 73
18. Tabor, D. and Winterton, R.S.H., "Surface Forces: Direct Measurement of Normal and Retarded van der Waals Forces", *Nature*, (1968), 219, 1120
19. Pfefferkorn, G. and Vahl, J., "Investigation of Corrosion Layers on Steel Using Electron Microscopy and Electron Diffraction", *Conf., Mechanism of Corrosion by Fuel Impurities*, p. 366, Marchwood, UK, Butterworths Publ., London, (1963)
20. Steel, J.S. and Brandes, E.A., "Growth and Adhesion of Oxides in Furnace Deposits and Their Influence on Subsequent Deposition of Ash Particles as Combustion Products", *Conf., Mechanism of Corrosion by Fuel Impurities*, p 374, Marchwood, UK, Butterworths, London, (1963)
21. Penney, G.W. and Klinger, E.H., "Contact Potentials and the Adhesion of Dust", *Trans. A.I.E.E.*, (1962), 81, 200
22. King, B.W., Tripp, H.P. and Duckworth, W.H., "Nature of Adherence of Porcelain Enamels to Metals", *Jour. Am. Cer. Soc.*, (1959), 42, 504
23. Holland, L., "The Properties of Glass Surfaces", Chapman and Hall, London, (1964)
24. Klomp, J.T., "Interfacial Reactions Between Metals and Oxides During Sealing", *Am. Ceram. Soc. Bull.*, (1979), 10, 887
25. International Critical Tables, "Surface Tension of Molten Sulphates", 4, 443, McGraw-Hill Book Co., New York, (1928)
26. Bertozzi, G. and Soldani, G., "Surface Tension of Molten Salts, Alkali Sulphate and Chloride Binary Systems", *Jour. Phys. Chem.*, (1967), 71, 1536
27. Raask, E., "Slag/Coal Interface Phenomena", *Trans. ASME for Power*, Jan., (1966), p 40
28. Cross, N.L. and Picknett, R.G., "Particle Adhesion in the Presence of Liquid Film", *Conf. Mechanism of Corrosion by Fuel Impurities*, p 383, Marchwood, UK, Butterworths, Publ., London, (1963)

29. Dietzel, A., "Explanation of Adhering Problem in Sheet Iron Enamels", Emailwaren-Industrie, (1934), 11, 161
30. Staley, H.F., "Electrolytic Reactions in Vitreous Enamels and Their Reaction to Adherence of Enamels to Steel", Jour. Am. Ceram. Soc., (1934), 17, 163
31. Weyl, W.A., "Wetting of Solids as Influenced by Polarizability of Surface Ions", Structure and Properties of Solid Surfaces, p 147, Edited by R. Gomer and C.S. Smith, University of Chicago Press, USA, (1953)
32. Oel, H.J. and Gottschalk, A., "The Adhesion Temperature Between Glass and Metals", Glastechnische Berichte, (1966), 39, 319
33. Raask, E., "Boiler Fouling - The Mechanism of Slagging and Preventive Measures", VGB Kraftwerkstechnik, (1973), 53, 248
34. Moza, A.K., Shoji, K. and Austin, L.G., "The Sticking Temperature and Adhesion Force of Slag Droplets from Four Coals on Oxidized Mild Steel", Jour. Inst. Fuel, (1980), 53, 17
35. Raask, E., "Mineral Impurities in Coal Combustion", Hemisphere Publishing Corp., New York, (1984)
36. Hodgman, C.D., (Editor), "Handbook of Chemistry and Physics", The Chemical Rubber Publishing Co., Ohio, USA, (1962)

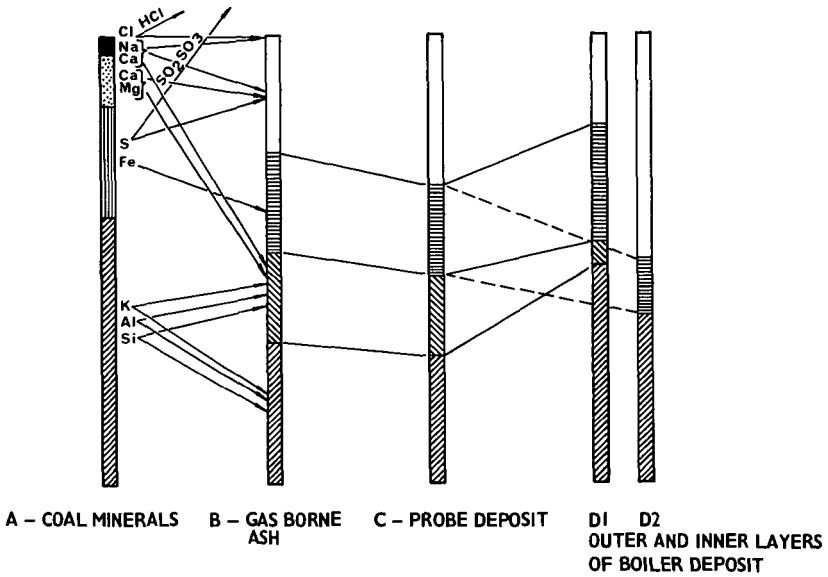


FIG. 1 ASH COMPOSITION CHANGES ON ROUTE FROM MINERAL MATTER TO BOILER TUBE DEPOSITS

- | | | |
|--|---|--|
|  IN SOLUBLE SILICATES |  SOLUBLE SILICATES | |
|  PYRITES |  IRON OXIDES |  CARBONATES |
|  CHLORIDES |  SULPHATES | |

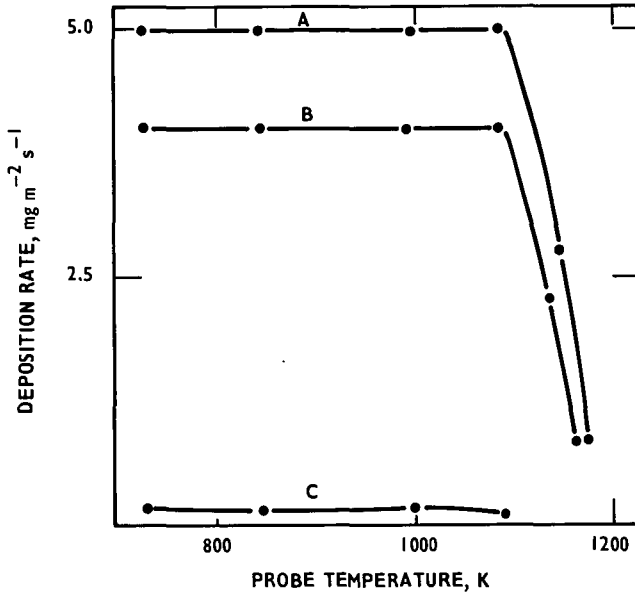


FIG. 2 DEPOSITION OF SULPHATE AND CHLORIDE IN
CYCLONE FIRED BOILER - 0.28 PER CENT
CHLORINE IN COAL

A - Na_2SO_4 B - K_2SO_4 C - NaCl

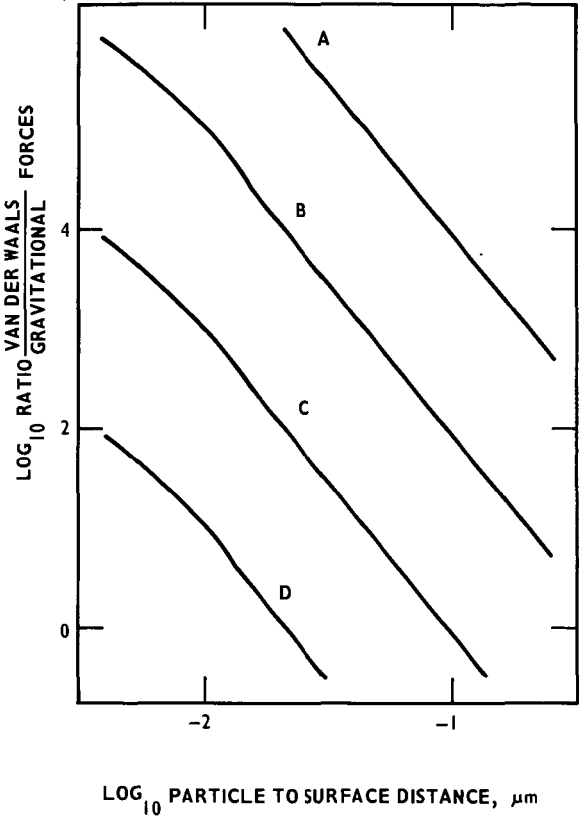
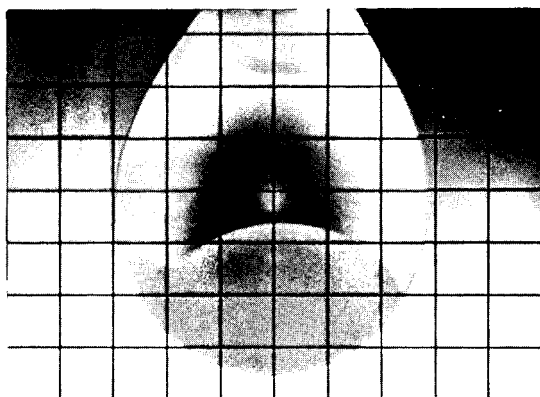


FIG. 5 COMPARISON OF VAN DER WAALS AND GRAVITATIONAL FORCES ON ASH PARTICLES NEAR COLLECTING SURFACES

PARTICLE DIAMETER, μm
A - 0.01; B - 0.1; C - 1.0; D - 10.0



TWO PHASES AT 1575K

FIG. 3 $2K_2SO_4 - K_2O - 2.1 SiO_2$ DROPLET IN HEATING MICROSCOPE (0.5 mm GRID)

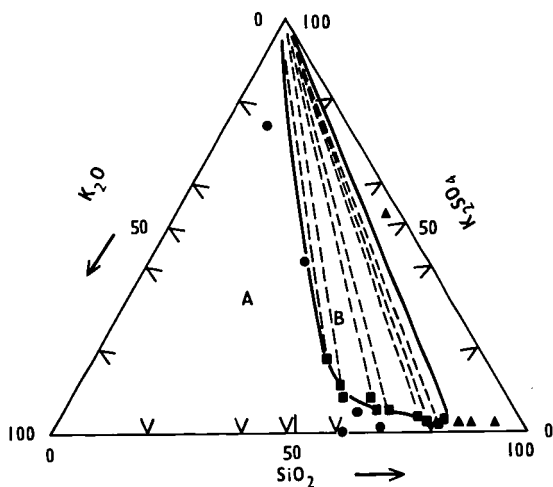


FIG. 4 MISCIBILITY GAP IN $K_2SO_4 - K_2O - SiO_2$ SYSTEM AT 1575 K
 A, SINGLE PHASE B, TWO PHASES C, LIQUID + SOLID SiO_2

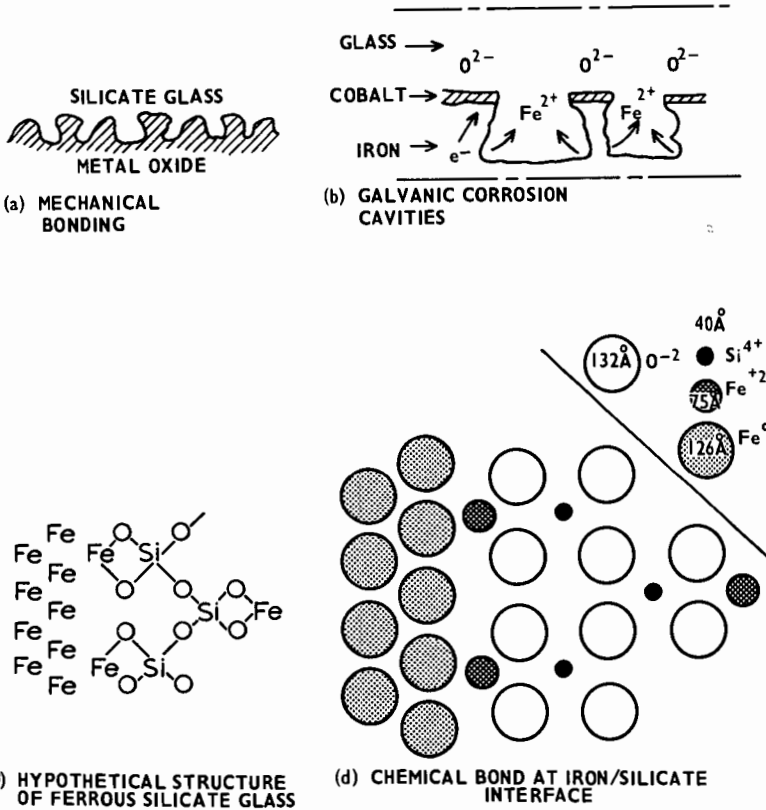


FIG. 6 SCHEMATIC REPRESENTATION OF MECHANICAL AND CHEMICAL BONDS AT BOILER TUBE/ASH DEPOSIT INTERFACE

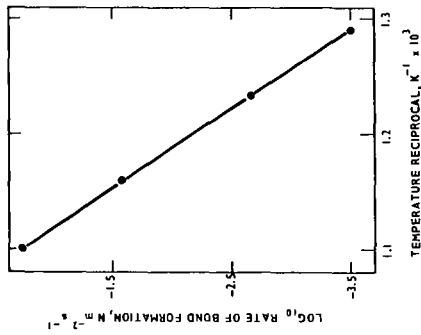


FIG. 7 THE EFFECT OF TEMPERATURE ON ASH DEPOSIT/FERRITIC STEEL BOND

ER/AWS(23.11.81)RL 4.3.3795

(R)

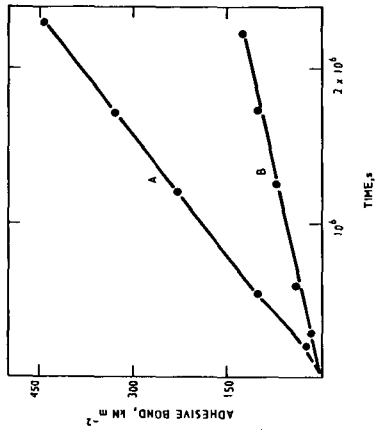


FIG. 8 BOND STRENGTH BETWEEN ASH DEPOSIT AND BOILER TUBE STEELS AT 900 K

A - FERRITIC STEEL

B - AUSTENITIC STEELS

ER/AWS(23.11.81)RL 4.3.3794

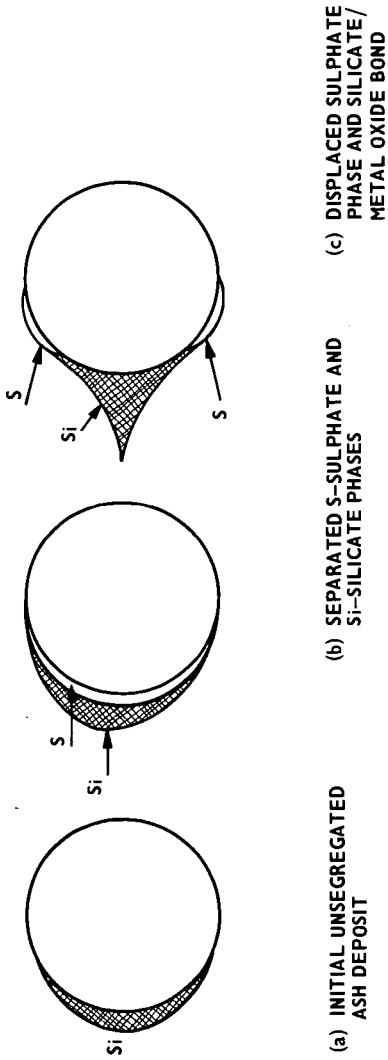


FIG. 9 SEQUENTIAL STAGES IN THE FORMATION OF LAYER-STRUCTURED AND FIRMLY
ADHERING SUPERHEATER DEPOSIT

USE OF GLASS FOR MODELING THE DEPOSITION OF
COAL ASH IN HOT CYCLONES

D. M. Mason and A. G. Rehmat

Institute of Gas Technology
IIT Center
3424 South State Street
Chicago, Illinois 60616

K. C. Tsao

University of Wisconsin — Milwaukee
P.O. Box 7841
Milwaukee, Wisconsin 53201

ABSTRACT

Tests have been conducted in a laboratory hot cyclone to obtain an estimate of the temperature below which spherical glass particles do not form a firmly attached deposit. A temperature of 800° to 850°C, corresponding to a viscosity between 6.3×10^5 and 2.9×10^6 poises, as calculated from the composition of the glass, was found. We take this viscosity to be approximately that of coal ash above which particles will not deposit in cyclones of fluidized-bed coal gasifiers.

INTRODUCTION

A cyclone operating at temperatures near those of the fluidized bed of the reactor has been used in the gasifier of the U-GAS® pilot plant to remove entrained char particles from the product gas and return them to the bed. Essentially pure coal ash has been found to deposit in this hot cyclone (1). The deposits have been analyzed chemically and examined by optical and scanning electron microscopy. Ferrous sulfide is responsible for deposition under adverse conditions, but deposition of iron-rich ferrous aluminosilicates is the more serious problem. In deposits from Western Kentucky coal, for example, the selective deposition of high-iron siliceous particles is indicated by an Fe_2O_3/Al_2O_3 ratio (calculated after excluding the iron contribution of iron sulfide) ranging from 2.2 to 4.6 in the ash of deposits, compared with a ratio of 1.2 in the ash of the coal. The effect of gas temperature (which equals particle temperature) and cyclone-wall temperature on the deposition of such particles was studied in a laboratory hot cyclone in the laboratories of the Mechanical Engineering Department of the University of Wisconsin at Milwaukee (1,2). The particles used in these tests were prepared from pilot plant deposits. The results indicated that the borderline temperature, below which the particles do not form a firm deposit, is about 900°C when gas and wall temperatures are equal.

We envision that the mechanism of deposition involves viscous or plastic flow following collision of particle and deposition surface to create a neck exerting enough surface tension to prevent rebound. We consider that the main cause of flow is impact. Flow driven by surface tension, as postulated by Raask (3) for deposition of coal ash on heat exchange surfaces of boilers, constitutes an additional mechanism leading to firm adhesion. Deposition at the inlet impingement area in the laboratory hot cyclone tests, massiveness of deposits at regions of high gas velocity and acceleration in or near the pilot plant cyclone, and virtual absence of deposits at low-gas-velocity regions of the gasification reactor all indicate that impact of deposition-prone particles plays an important role in the mechanism.

For both mechanisms, however, the effect of temperature on deposition can be attributed to change in viscosity, as surface tension does not vary much with temperature. Investigation of the effect of viscosity with ash particles is difficult, because little is known about the viscosities of iron aluminosilicates and ferrous sulfide at temperatures from 850° to 1050°C and, in any case, the ash particles vary in composition and presence of high melting phases. Therefore, we have chosen to use glass spheres as a homogeneous model material of known viscosity for the study of deposition. We report here a few results of a preliminary nature.

EXPERIMENTAL

The test apparatus consists of a natural gas burner to provide hot flue gas, a dust feeder, and a 9.68-cm ID cyclone (Figure 1). Calculations indicate that the residence time of particles in the hot flue gas is sufficient to heat the particles to the temperature of the flue gas at the cyclone entrance. The inlet section of the cyclone is jacketed to allow cooling of the wall; or alternatively, it can be heated to achieve substantially equal gas and wall temperatures. Temperature readings of the gas during a run are taken by a bare wire thermocouple projecting into the gas just upstream from the inlet section of the cyclone; it is calibrated before the run by an aspiration thermocouple in the inlet section. Temperature of the wall is measured by a thermocouple embedded in it at the spot where the entering gas impinges, where coherent deposits typically form (1,2). The surface of the inlet section is smoothed with No. 320-grit emery paper before each test.

The feed dust in these tests was supplied by the Cataphote Division of Ferro Corporation as Class IV-A uncoated Unispheres of soda-lime glass in a nominal 13-44 μm diameter. A Coulter counter size distribution analysis indicated that the size ranged only between 20 and 51 μm , with 14% greater than 40 μm and 3% smaller than 25 μm .

To determine the borderline of deposition we have made a total of nine runs with the glass spheres, of which seven were within about 50°C of a borderline region obtained by plotting wall temperature against gas temperature (Figure 2). The burner was operated to yield an oxidizing atmosphere at rates giving cyclone inlet velocities ranging from 30 to 50 f/s; these velocities are comparable to those of laboratory tests with particles of pilot plant deposits. Very light but firm deposits of the spheres were observed at the jet impingement area in three of these tests. The results indicate that the borderline for firm deposition with equal gas and wall temperatures is between 800° and 850°C. The slope of the borderline, which should depend mostly on the specific heat of the dust, is assumed to be parallel to the better-established borderline for the pilot plant deposits, which is also shown in Figure 2. In the future, we expect to make additional tests to establish the borderline more precisely and to determine the effect of variables such as velocity and size of particles.

We have chemically analyzed the glass spheres and from this estimated the viscosity at 800° and 850°C by means of the correlation equations of Lyon (4,5). The range of viscosity thus obtained over the above temperature range is 6.3×10^5 to 2.9×10^6 poises. This is near the geometric mean of the viscosities at the softening and working temperatures of glass (5).

DISCUSSION

According to Dietzel's correlation of the surface tension of glasses, glazes, and enamels with composition (6), the surface tension of the pilot plant deposits is up to about 25% higher than that of the glass used here. Neglecting this difference and the effect of particle shape, we may conclude that the effective viscosity of the pilot plant deposit for borderline deposition in the laboratory hot cyclone is in the range reported above for the glass spheres. In the pilot plant or in a commercial plant with much larger cyclones, considerable scale-up is required for application of our results, but we think it likely that they apply there also.

REFERENCES CITED

1. Mason, D. M.; Rehmat, A.; Tsao, K. C. "Chemistry of Ash Deposits in the U-GAS Process." In Fouling of Heat Exchange Surfaces, Bryers, R. W., Ed. Engineering Foundation: New York, 1983.
2. Tsao, K. C.; Tabrizi, H.; Rehmat, A.; Mason, D. M. "Coal-Ash Agglomeration in a High-Temperature Cyclone," Am. Soc. Mech. Eng. [Pap], ASME Annual Meeting, November 1982, ASME Preprint No. 82-WA/HT-29.
3. Raask, E. VGB Kraftwerkstechnik 1973, 53(4), 248.
4. Lyon, K. C. J. Res. Nat. Bur. Stand. Section A, 78A, 1974, 497.

5. Boyd, D. C.; Thompson, D. A. "Glass," in Encyclopedia of Chemical Technology, 11, 807-80. Wiley: New York, 1980.
6. Scholze, H. "Glas-Natur, Struktur and Eigenschaften," 213-21. Vieweg: Braunschweig, 1965.

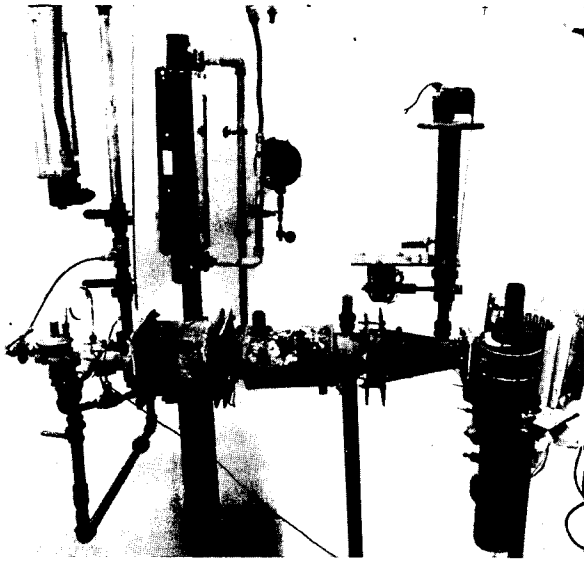


Figure 1. LABORATORY HOT CYCLONE APPARATUS

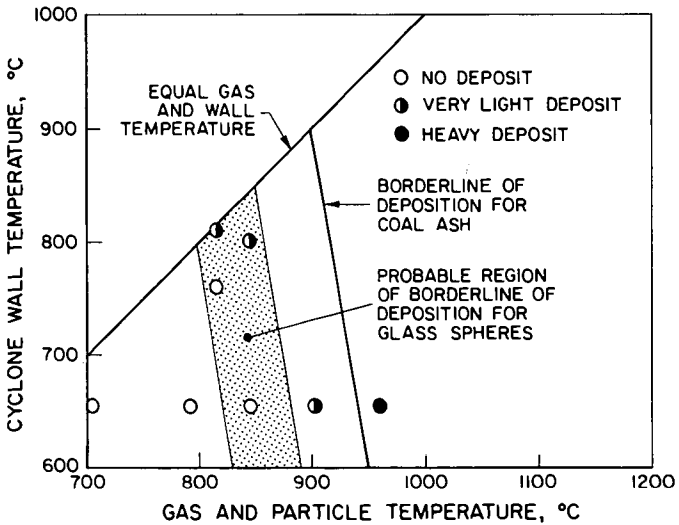


Figure 2. BORDERLINE OF DEPOSITION

A83111582

A STUDY OF SLAG DEPOSIT INITIATION IN A DROP-TUBE TYPE FURNACE

Murray F. Abbott* & Leonard G. Austin

Fuel Science Section and Department of Mineral Engineering
The Pennsylvania State University
University Park, PA 16802

ABSTRACT

A drop-tube furnace was designed and constructed for the purpose of simulating the time/temperature environment for p.c. combustion in a utility furnace. The ash produced was impacted on oxidized boiler steel coupons at gas and metal temperatures similar to upper furnace waterwall tubes. Both fly ash and deposits were similar to those of a pilot-scale (7-9 kg/hr) combustor. Iron-rich slag droplets produced from pyrite-rich p.c. particles bonded strongly with the oxidized steel surface. These particle types were found at the base of ash deposits after removal of sintered and loose ash for both eastern and western coals. Adhesion of iron-rich droplets was a function of both flame and metal surface temperatures. Also, volatile species, i.e., alkali and exchangeable cations influenced the "sticking" behavior of the iron-rich droplets. These trends are in qualitative agreement with previous sticking test results.

INTRODUCTION

All coals contain inorganic matter which is converted to ash when the coal is burned. The management of this ash constitutes one of the principal limiting design considerations for a p.c. steam generator. Operational problems occur if ash deposition and build-up on heat exchange surfaces becomes unmanageable. A single day's outage for an 800 MW unit for ash removal and repair can cost the utility as much as \$600,000 in lost electrical generation (1). Derating of the boiler system to manage ash deposition problems can cost millions of dollars annually. This investigation is part of an ongoing research program to gain a better fundamental understanding of the initiation of slag deposits on the upper walls of a boiler furnace enclosure. This paper reports on the development of a gas-fired vertical muffle tube (drop-tube) furnace as a new research tool.

A previous laboratory test, the sticking test (2-7) led to a number of conclusions concerning the mechanism and chemistry of molten slag drop adhesion to oxidized boiler steels. However, this test had several inherent disadvantages. It required the use of comparatively large molten ash drops (2 mm in diameter) and there was no proof that the conclusions applied equally well to the smaller size droplets (submicron to 250 μ m) produced in p.c.-fired furnaces. Also, the large drops formed from a coal ash contained all of the constituents of the ash (mean ash composition) which cannot accurately simulate the variety of mineral associations occurring on a particle-by-particle basis in a pulverized coal (8). Thus, the purpose of the drop-tube furnace was to produce coal fly ash particles under the same time/temperature environment experienced in full-scale boiler combustion followed by impaction on an oxidized boiler steel coupon simulating an upper furnace waterwall surface.

EXPERIMENTAL

Three Pennsylvania bituminous coals, designated Keystone, Montour and Tunnelton and a Decker, Montana subbituminous coal were studied in this investigation. All are current steam coals. Semi-quantitative mineralogical analysis of LTA and spectrochemical analysis of ASTM HTA are given in Table 1 for the three

*Current Address: Babcock & Wilcox R&D, 1562 Beeson Street, Alliance, OH 44601

Pennsylvania coals and raw (untreated) and acid washed Decker coal samples.

The drop-tube furnace system in which the test coals were burned is shown in Figure 1. It consisted of four major component parts: (i) a gas-fired hot zone, (ii) a fluid-bed feeding system, (iii) a preheat section and injector, and (iv) a water-cooled ash collector probe. The conditions inside the heated muffle tube simulated those of a utility furnace combustion zone: (i) maximum gas temperatures of 1500 to 1750°C, (ii) particle residence times between one and two seconds, and (iii) ash sampling temperatures ranging from 1000 to 1300°C. The fluid-bed feeder delivered between 0.2 and 0.3 grams of pulverized coal with slightly less than 1 liter of primary air per minute. In the preheat section the secondary air stream (roughly 2 liters/min) was heated to about 1000°C before a honeycomb flow straightener distributed it in streamlines across the muffle tube cross-section. The cold p.c./primary air mixture was carried by the injector to the hot combustion zone. A thin pencil-like p.c. stream was burned as it passed through the heated muffle tube. The fly ash produced was accelerated and impacted onto a water-cooled boiler steel coupon at surface temperatures of 300 to 450°C.

The ash deposits were characterized physically by observation under both a Zeiss optical and IDS-130 scanning electron microscope (SEM). Chemical characteristics were determined by energy dispersive x-ray fluorescence equipment associated with the SEM.

RESULTS AND DISCUSSION

Physical characteristics for all ash deposits were similar. Figure 2 shows a typical ash deposit structure on both a macro and microscale. The top photograph (A) shows an ash deposit collected from the raw Decker coal on a Croloy 1/2 steel coupon. The lower optical photomicrograph shows the strongly bonded material remaining on the surface after the comparatively loosely adhered ash had been brushed away. The opaque black droplets are rich in iron (85 to 100 wt. %) and the light colored transparent glassy spheres are predominantly aluminosilicates. The deposit build-up mechanism appeared to be similar for all coals. All originated with the relatively strong bonding of iron-rich slag drops to the oxidized steel surface. Aluminosilicates were only found in this layer for the raw Decker coal. In addition, there was always a layer of very fine particles (submicron) covering the entire coupon surface. It was not possible to brush or blow this layer from the surface. A region of loosely bonded ash particles often containing most all of the major constituents of the ash then built upon the more strongly adhered droplets. There was little if any interaction between the loose ash and adhesive particles. As the distance from the steel surface increased the ash particles began to sinter, eventually forming a fluid mass in some instances.

Preferential deposition of iron-rich species has been suggested by other investigators (9,10). It was also observed in a pilot-scale p.c. test combustor (11). The fine particle layer probably formed on the coupon surface due to convective diffusion to the relatively cold steel coupon (12). Presumably the scouring action of the ash laden gases in a utility furnace would prevent formation of the loose ash layer until the iron-rich layer is more extensively developed and interaction with successive layers can occur.

The iron-rich deposit base particles formed from the Keystone coal at flame temperatures of 1470 (A) and 1500°C (B) are shown in the SEM photomicrographs in Figure 3. The concentration of these particles increased with increasing flame temperature. Note that the particles flattened more on impact at the higher temperature, probably due to a decrease in particle viscosity. There appeared to be two different iron-rich particle types in each deposit: (i) a porous particle with a rougher surface texture, and (ii) a more glassy appearing particle with a very smooth surface texture. X-ray fluorescence spectrograms are also shown in Figure 3. The porous type particles were found to contain exclusively iron (see analysis of Point 1 in Figure 3B), whereas the more glassy particle types contained smaller amounts of silicon, aluminum and potassium (Point 2).

The two furnace operating parameters which most influenced ash deposition rates

were flame and coupon surface temperatures. Both of these trends are shown in Tables 2 and 3. Deposit build-up rates increased between two and six times with each increase in flame temperature and ten-fold for a 30 degree rise in coupon surface temperature. Removing exchangeable cations from the Decker coal caused a three-fold decrease in the ash deposition rate, see Table 4. The exchangeable cations appeared to play a significant role in both the initial iron-rich deposit and the sintering properties exhibited by the ash deposit. The sintered ash collected from the raw Decker coal was yellow-brown in color and comparatively difficult to break apart requiring a force of nearly 20 psi. The acid form sinter was coral colored and broke apart while removing the coupon from the collector probe.

CONCLUSIONS AND FUTURE WORK

The drop-tube furnace closely simulated the time/temperature history of a utility boiler furnace. One type of slag deposit initiating particle which strongly bonds to oxidized boiler steels is low melting iron-rich droplets produced from pyrite-rich p.c. particles. Flame and metal surface temperatures strongly influence ash deposit build-up rates. Sufficient evidence exists to suggest that alkalis and calcium enhance the "sticking" behavior of iron-rich and other fly ash droplets. This investigation revealed a qualitative relationship between results obtained from several different apparatus used to study slag initiation: (i) sticking apparatus, (ii) drop-tube furnace, and (iii) pilot-scale p.c. test combustor.

Future work in the drop-tube furnace will include: (i) developing a method for defining the relative adhesion properties of ash particle types, and (ii) more clearly defining the role of volatile species in deposit initiation and growth. This second goal can be accomplished by investigating controlled composition synthetic polymer/mineral combinations.

ACKNOWLEDGEMENTS

This study was funded by grants from the Department of Energy, Contract No. DE-FG22-80PC-30199 and Babcock and Wilcox.

REFERENCES

- 1) Williams, N., Sharbaugh, R., Van Tiggerler, D. and Kadlec, R., Electric Light and Power, 25 (1983).
- 2) Moza, A.K. and Austin L.G., Fuel, 60, 1057-64 (1981).
- 3) Abbott, M.F., Moza, A.K. and Austin, L.G., Fuel, 60, 1065-72 (1981).
- 4) Moza, A.K. and Austin, L.G., Fuel, 61, 161-5 (1982).
- 5) Abbott, M.F. and Austin, L.G., Fuel, 61, 765-70 (1982).
- 6) Abbott, M.F., Conn, R.E. and Austin, L.G., "Studies on slag deposit formation in pulverized coal combustors. 5. The effect of flame temperature, thermal cycling of the steel substrate, and time on the adhesion of slag drops to boiler steels", in preparation.
- 7) Abbott, M.F. and Austin, L.G., "Studies on slag deposit formation in pulverized coal combustors. 6. The sticking behavior of slag from three Pennsylvania steam coals", in preparation.
- 8) Moza, A.K., Austin, L.G. and Johnson, G.G., Jr., SEM/1979/1, p. 473, SEM Inc, AMF O'Hare, IL, 1979.
- 9) Borio, R.W. and Narcisco, R.R., Journal of Engineering for Power, 101, 500 (1979).
- 10) Bryers, R.W., Journal of Engineering for Power, 101, 517 (1979).
- 11) Austin, L.G., Abbott, M.F. and Kinneman, W.P., Jr., ASME 83-JPGC-Pwr-42.
- 12) Rosner, D.E., Chen, B.K., Fryburg, G.C. and Kohl, F.J., Combustion Science and Technology, 20, 87-106 (1979).

TABLE 1. MINERALOGICAL AND ELEMENTAL ASH COMPOSITION FOR TEST COALS

<u>Procedure/Coals</u>	<u>Montour</u>	<u>Keystone</u>	<u>Tunnelton</u>	<u>Raw Decker</u>	<u>Acid-Washed Decker</u>
Mineralogical (wt. % LTA)					
Quartz	25	25	22	20	30
Pyrite	15	10	15	5	10
Calcite	5	--	5	5	--
Gypsum	--	5	--	30	--
Kaolinite	17	30	18	11	16
Illite	30	20	30-40	--	--
Feldspan	--	--	5-10	--	--
LTA (wt. % as received coal)	18.0	21.6	22.9	6.3	3.3
HTA (wt. % as received coal)	15.8	18.0	20.1	4.0	2.2
Spectrochemical (wt. % HTA)					
SiO ₂	51.7	54.1	50.3	26.5	53.0
Al ₂ O ₃	25.6	25.9	26.8	15.5	28.5
TiO ₂	1.3	1.3	1.3	0.9	2.7
Fe ₂ O ₃	14.1	9.7	11.0	5.3	9.2
CaO	2.4	1.8	2.5	14.3	4.1
MgO	0.9	1.0	1.0	2.5	0.7
Na ₂ O	0.2	0.3	0.4	0.03	0.01
K ₂ O	2.4	2.9	2.9	5.0	0.4
SO ₃	1.5	1.1	2.3	0.97	0.6
P ₂ O ₅	0.4	0.4	0.4	21.6	--

TABLE 2. DEPOSIT BUILD-UP RATES FOR THE THREE PENNSYLVANIA STEAM COALS AT THREE FLAME TEMPERATURES

Coal	Flame Temperature °C	Deposit Mass mg	Relative Build-up Rates		Percent of Total Ash (Based on HTA)
			mg/min	mg/gr Coal	
Montour	1465	26.5	2.2	11.0	6.9
	1518	64.5	5.4	22.5	14.2
	1561	133.0	11.1	46.3	29.2
Keystone	1470	24.0	2.0	7.1	3.9
	1500	117.7	9.8	40.8	22.7
	1560	286.1	23.8	99.2	47.3
Tunnelton	1467	39.7	3.3	11.8	3.1
	1510	252.6	21.1	75.4	19.7
	1518	297.1	24.8	103.3	51.3

TABLE 3. DEPOSIT BUILD-UP RATES FOR THE KEYSTONE COAL AT A FLAME TEMPERATURE OF 1500°C AND TWO DIFFERENT COUPON SURFACE TEMPERATURES

Coupon Surface Temperature °C	Deposit Mass mg	Relative Build-up Rates		Percent of Total Ash (Based on HTA)
		mg/min	mg/gr Coal	
310-318	11.7	6.98	29.1	2.3
340-345	117.7	9.8	40.8	18.0

TABLE 4. DEPOSIT BUILD-UP RATES FOR RAW AND ACID WASHED DECKER COAL SAMPLES AT A FLAME TEMPERATURE OF 1500°C

Coal Sample	Deposit Mass mg	Relative Build-up Rates		Percent of Total Ash (Based on HTA)
		mg/min	mg/gr Coal	
Raw Decker	82	4.1	14.6	36.6
Acid Washed Decker	25	1.3	5.4	23.7

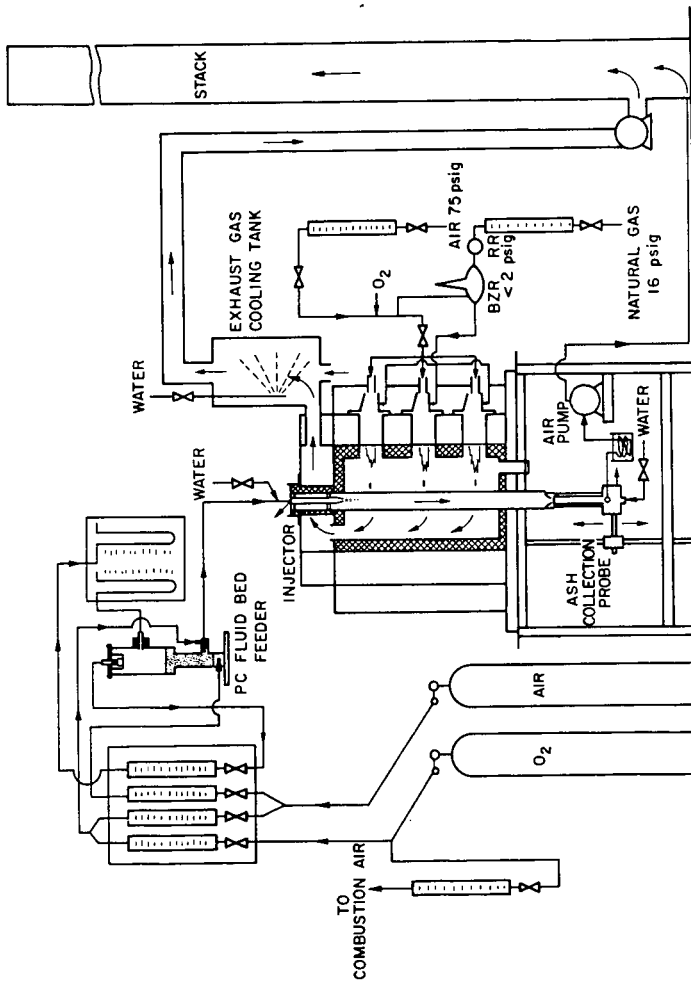
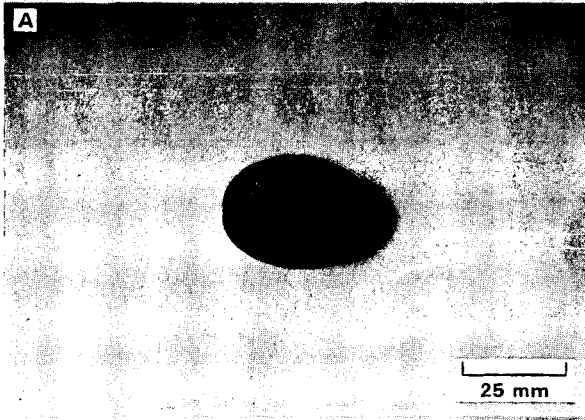


FIGURE 1 DROP-TUBE FURNACE SYSTEM



**FIGURE 2 RAW DECKER COAL ASH DEPOSIT:
A) TOTAL DEPOSIT AFTER TWENTY MINUTES,
B) OPTICAL PHOTOMICROGRAPH OF BONDED
ASH PARTICLES**

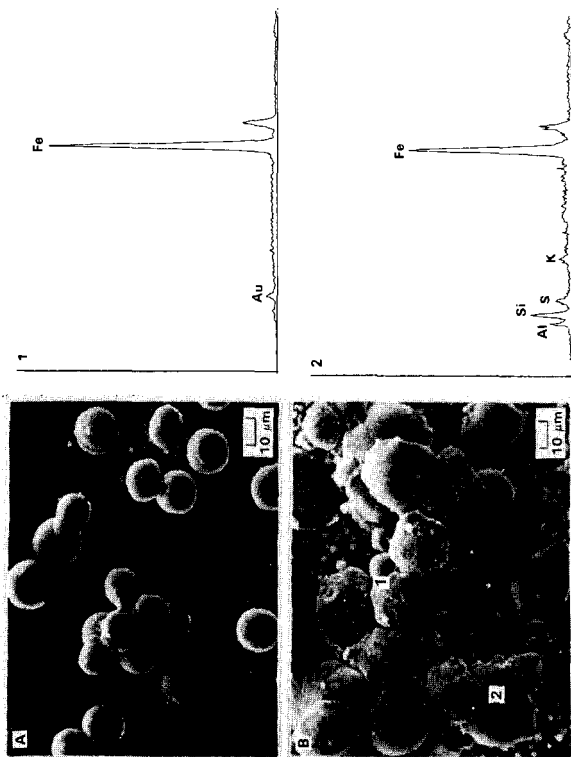


FIGURE 3 KEYSTONE COAL ASH DEPOSITS: A&B) SEM PHOTOMICROGRAPHS SHOWING IRON-RICH SLAG DROPLETS COLLECTED FROM FLAME TEMPERATURES OF 1470°C (A) AND 1550°C (B). X-RAY FLUORESCENCE SPECTROGRAMS CORRESPONDING TO POINTS 1 AND 2 IN PHOTO B.

INFLUENCE OF SEGREGATED MINERAL
MATTER IN COAL ON SLAGGING

R. W. Bryers

Foster Wheeler Development Corporation
12 Peach Tree Hill Road
Livingston, New Jersey 07039

INTRODUCTION

The mineral content of any given rank of coal is a key factor in sizing and designing a steam generator or reactor. The mineral content becomes even more important as the premium solid fuels are consumed, leaving reserves with continual increasing mineral concentrations and lower quality ash. The problem of dealing with lower quality ash in coal is compounded by the increase in size of steam generators and refinements imposed by economic constraints. Empirical indices, based on coal ash chemistry and ASTM ash fusion temperatures or viscosity, are presently used to rank coals according to the fireside behavior of the mineral matter. Unfortunately, the indices are only marginally satisfactory, as they do not relate to operating or design parameters and frequently are based on a coal ash chemistry quite different from that deposited on the furnace wall. Frequently, different coals with identical ash chemistry produce decidedly different slagging conditions in steam generators of identical design operated in the same mode. Variations in composition of the slag, when compared with the coal ash, suggest specific minerals are being selectively deposited on furnace walls depending upon their specific gravity, size, composition, and physicochemical properties. It is quite apparent there is a need for a better understanding of the impact of mineral composition, its size, and its association with other minerals and carbonaceous matter on fireside deposits.

MINERAL MATTER IN COAL

Minerals occurring in coal may be classified into five main groups. These include shale, clay, sulfur, and carbonates. The fifth group includes accessory minerals such as quartz and minor constituents like the feldspars (1).

Shale, usually the result of the consolidation of mud, silt, and clay, consists of many minerals including illite and muscovite--these are forms of mica. Kaolinite is the most common clay material (1).

The sulfur minerals include pyrites with some marcasite. Marcasite has the same chemical composition as pyrites but a different mineralogical structure. Sulfur is also present as organic matter and occasionally as sulfate. The latter usually occurs in weathered coal such as in outcrops. The amount of sulfate sulfur in coal is generally less than 0.01 percent.

Generally, 60 percent of the sulfur in coal is pyritic, particularly when the sulfur concentration is low. At higher concentrations it may run as high as 70 to 90 percent. Pyrite occurs in coal in discrete particles in a wide variety of shapes and sizes. The principal forms are (1-6):

- Rounded masses called sulfur balls or nodules an inch or more in size.
- Lens-shaped masses which are thought to be flattened sulfur balls.
- Vertical, inclined veins or fissures filled with pyrite ranging in

thickness from thin flakes up to several inches thick.

- Small, discontinuous veinlets of pyrite, a number of which sometimes radiate from a common center.
- Small particles, 72μ, or veinlets disseminated in the coal. Microscopic pyrite occurs in five basic morphology types: (a) framboids, (b) isolated euhedral crystals, (c) nonspherical aggregates of euhedral crystals, (d) irregular shapes, and (e) fractured fillings (7).

All coals contain some of the third and fifth forms of pyrite, and some coals contain all five of the principal forms (6,8,9).

The carbonates are mainly calcite, dolomite, or siderite. The occurrence of calcite is frequently bimodal. Some calcite occurs as inherent ash, while other calcite appears as thin layers in cleats and fissures. Iron can be present in small quantities as hematite, ankerite, and in some of the clay minerals such as illite. In addition to the more common minerals, silica is present sometimes as sand particles or quartz. The alkalis are sometimes found as chlorides or as sulfates but probably most often as feldspars, typically orthoclase and albite. In the case of lignites, unlike bituminous and subbituminous, sodium is not present as a mineral but is probably distributed throughout the lignite as the sodium salt of a hydroxyl group or a carboxylic acid group in humic acid. Calcium, like sodium, is bound organically to humic acid. Therefore, it too is uniformly distributed in the sample.

The term, "mineral matter," usually applies to all inorganic, noncarbonaceous material in the coal and includes those inorganic elements which may occur in organic combination. Physically, the inorganic matter can be divided into two groups--inherent mineral matter and extraneous mineral matter. Inherent mineral matter originates as part of the growing plant life from which coal was formed. Under the circumstances, it has a uniform distribution within the coal. Inherent mineral matter seldom exceeds 2 - 3 percent of the coal (10).

Extraneous mineral matter generally consists of large bits and pieces of inorganic material typical of the surrounding geology. In some cases the extraneous matter is so finely divided and uniformly dispersed within the coal it behaves as inherent mineral matter. Coal preparation can separate some of the extraneous ash from the coal substance, but it seldom removes any of the inherent mineral matter.

The physical differences between inherent and extraneous ash are important not only to those interested in cleaning coal but also to those concerned with the fire-side behavior of coal ash. Inherent material is so intimately mixed with coal that its thermal history is linked to the combustion of the coal particle in which it is contained. Therefore, it will most likely reach a temperature in excess of the gas in the immediate surroundings. The close proximity of each species with every other species permits chemical reaction and physical changes to occur so rapidly that the subsequent ash particles formed will behave as a single material whose composition is defined by the mixture of minerals contained within the coal particle. The atmosphere under which the individual transformations take place will, no doubt, approach a reducing environment. Figure 1 illustrates a model of the coal and mineral matter as fed to the combustor and the fate of the minerals after combustion (11).

Extraneous materials can behave as discrete mineral particles comprised of a single species or a multiplicity of species. As already indicated, a portion of this material may be so finely divided it can behave as inherent mineral matter.

During combustion the larger particles respond individually to the rising temperature of the environment. In the absence of carbon or other exothermic reactants, the particle should always be somewhat less than the local gas temperature. However, the particles may be subjected to either reducing or oxidizing conditions. As each particle rises in temperature, it loses water of hydration, evolves gas, becomes oxidized or reduced, and eventually sinters or melts, depending on its particular composition or temperature level.

It is evident, then, that there can be a great difference in the final state of each particle, depending upon its composition and whether it is inherent or extraneous ash. Figure 2 summarizes the phase transformations which pure mineral matter commonly found in coal undergoes during heating (12,13,14). Since this data was developed primarily by mineralogists performing differential thermal analysis under air at slow heating rates, it must be used only as a guideline for predicting the thermal behavior of minerals in coal. Thermal shocking these minerals in the presence of carbon and other mineral forms at very high temperatures, no doubt, will alter some of these transformations and may defer others until postcombustion deposition on heat transfer surfaces.

Clays and Shale

The melting temperatures of most pure minerals are in the vicinity of or greatly exceed the maximum flame temperature encountered during combustion. Therefore, the fused spheroidal fly ash, generated from the mineral matter in coal, primarily forms as the result of the fluxing action between pure minerals contained within each particle. Illite and biotite appear to be an exception. Both minerals contain small concentrations of iron and potassium and form a glassy phase at 950°C and 1100°C, respectively. Depending upon its fluidity, this glassy phase could be responsible for surface deformation at a relatively low temperature and provide the necessary sticking potential to prevent reentrainment upon contacting heat transfer surfaces. Low temperature ash of a gravity fraction containing illite was heated in a thermal analyzer under air to 600 and 1000°C, respectively, and compared to the low temperature ash of a gravity fraction void of illite. The scanning electron photomicrographs, appearing in Figure 3, indicate the minerals containing illite did, indeed, show signs of the formation of a melt.

Quartz

The inherent silica retained in the char as quartz or silica released from kaolinite and illite at low temperatures (i.e., 950°C) is partially reduced to silica monoxide. Unlike silica which boils at 2230°C, silica monoxide melts at 1420°C and boils at 2600°C (15). The vapor pressure of silicon is low--in the range of temperatures experienced during combustion. Honig reports values ranging from 0.01m Hg at 1157°C to 1m Hg pressure at 1852°C (15,16). The presence of other mineral matter and carbonaceous material appears to alter vapor pressure substantially. When a mixture of alumina silicate and graphite was heated, the volatilization of silicon monoxide began at about 1150°C and reached a maximum at 1400°C. Mackowsky reports that volatilization of silicon monoxide starts at about 1649°C in the presence of carbonates and clays and reaches a maximum at 1704°C (17). In the presence of pyrite or metallic iron, volatilization begins at about 1560°C and continues at a rapid rate as the temperature rises until practically all the silica in the mineral is volatilized. Sarofin has shown that about 1.5 to 2.0 percent of the ASTM ash in bituminous coals volatilize (18). Approximately 35 - 40 percent of the volatilized material was silica. The next largest component was iron. Extraneous quartz appears to be relatively innocuous unless contaminated by Fe₂O₃, CaO, or K₂O.

Pyrites

The decomposition of pyrite has been examined by numerous investigators under oxidizing, neutral, and reducing environments. TGA, rather than DTA, has been used by most investigators. Acquisition of representative data is difficult, as the decomposition process is complex and sensitive to many variables including the chemical composition of pyrites, its grain size, its origin, the presence of adventitious impurities, the composition of the local environment, and diffusion rates through sulfated layers. Under oxidizing conditions it is believed that pyrites decompose directly to an iron oxide and SO_2 or SO_3 or iron sulfate and SO_2 , depending upon the final temperature level. Under reducing conditions pyrrhotite and either carbon or hydrogen sulfide form. Complete reduction results in elemental iron and carbon disulfide. There is also a possibility that pyrrhotite may form under oxidizing conditions as an intermediate step in the presence of sufficient adventitious carbon. Pure pyrites ignite at about 500°C in the thermal analyzer at $20^\circ\text{C}/\text{min}$ and burn out by 550°C in a single-step process, as shown in Figure 5. Pure pyrites do ignite as readily as bituminous coal; however, the burnout time is comparable. Although pyrrhotite ignites readily, it requires as much time as anthracite to complete combustion. Pyrites containing small quantities of adventitious carbon, as might be found in the -1.80 $+2.85$ gravity fraction, appear to form pyrrhotite, deferring burnout until 800°F . Within the combustor the problem is compounded by the fact that pyrite particles do not shrink during the combustion process as do coal particles, and hence, their burnout time is extended. The burnout time of particles in excess of 40μ appears to exceed the residence time available in most combustors.

TGA reveals decomposition rates but tells little about the physical state during the combustion process. Phase diagrams for the Fe-S-O and FeS-FeO system, representing transitory states at the particle surface, imply the formation of a temporary melt at low temperatures. SEM photomicrographs, appearing in Figure 5, of pure pyrites heated to 600°C , 800°C , and 1000°C under reducing conditions clearly reveal the formation of a melt at temperatures as low as 600°C . Large particles of partially-spent pyrites, which may be molten on contact with the heat transfer surface, complete the oxidation process in situ, forming a solid fused deposit with a very high melting temperature.

An examination of the thermal behavior of the mineral matter in coal indicates the mineral origin of the elements found in coal ash and their juxtaposition with regard to each other, as well as other mineral forms, and determines their physical fate during combustion. As indicated in Figure 1, the physical state (i.e., vapor or solid) and the size of solidified ash will determine the mode and rates of migration to the heat transfer surface. The physical state at the tube surface will depend upon the local surface temperature and the composition of the particulate depositing. In the case of pyrites residence time and environment conditions may also play a significant role.

CHARACTERIZATION OF MINERALS IN COAL

The fireside behavior of mineral matter in coal has been investigated by characterizing the mineral content of several bituminous coals, using size and gravity fractionation analysis of pulverized coal and then firing the coal in a vertically fired combustor. High sulfur coals containing pyrites of varying size and varying association with carbonaceous and other mineral forms were selected for examination. A comparison was also made with western subbituminous coals to assess the impact of potassium in the mineral illite on furnace slagging.

Each coal was analyzed for proximate, ultimate, ash chemistry, and ash fusion temperatures to permit evaluation using conventional data. The pulverized coal samples were then divided into four sizes representing equal weights (i.e., +105 μ , -105 μ +74 μ , -74 μ +44 μ , and -44 μ). Each size fraction was separated into four weight classes, thereby, partitioning the coal into groups dominated by coal, non-pyritic mineral matter, and pyrites. The partitioned coal was analyzed for ash chemistry, ash fusion temperature, combustion profile, and mineral content.

The analytical data is summarized in Figure 6. The enclosed data points represent the composite analysis. The open data points represent the fractionated species. Ash softening temperatures and percent basic constituents were selected as the variables to characterize the coal, as they appear most frequently in the indices used to express the slagging or fouling potential of the fuel. It is quite evident the combustor is exposed to ash with a wide range of chemical compositions and melting temperatures not adequately identified by a composite coal analysis. The data indicates slagging was most severe with coals having the highest melting temperature and demonstrating the greatest degree of separation of ash from coal and pyrites from other mineral matter. The two coals with the lowest composite ash softening, having the highest slagging index by conventional evaluation, caused the least slagging. Liberation of mineral matter from these two coals was also the lowest.

The data was replotted on fusibility diagrams, appearing in Figure 7, typifying the coal with the greatest partitioning of mineral matter and highest degree of slagging and the coal with the least liberation of mineral matter and degree of slagging. The fusibility diagram illustrates the size and weighted contribution of each ash specie. It also shows the degree of liberation of nonpyritic and pyritic mineral matter. By washing the worst coal at 1.80 sp. gr. and 14M x 0, thereby minimizing extraneous ash as well as total sulfur, the degree of slagging of the Upper Freeport coal was greatly reduced.

COMBUSTION TESTING

Deposits were removed from various locations in the combustor after firing each coal for \approx 14 - 16 hours. Samples were removed from slagging probes at 398 - 510°C, fouling probes at 510 - 537°C, and refractory surfaces at 537 - 1204°C and examined using the scanning electron microscope and energy dispersive x-ray. Fly ash samples were also examined for carbon loss, surface morphology, and chemical composition.

The deposits forming on the slagging probes were initiated by a thin layer of powdery fly ash, <8 μ in size, enriched with small quantities of potassium. Beads of slag formed on top of this thin layer when the surface temperature approached the initial deformation temperature of the deposit. Growth progressed with the formation of rivulets from which a continuous phase of molten slag formed. Deposits forming on the refractory surface represent an advanced stage of slag due to the higher surface temperatures which could only be achieved on the cooler probes after the initial dust layer formed. The composite ash chemistry and ash fusion temperatures of the slag resemble that of the heaviest gravity fraction (i.e., >1.80 sp. gr.) in most cases. Macro photographs of the deposit formation on the furnace probes subjected to axial symmetric flow at low gas velocities (5 - 6 ft/s), illustrated in Figure 8, show that the initial layer of dust, upon which further slagging depends, formed only when firing coals whose ash contained more than 1 percent potassium. Continued deposit growth resulting in serious slagging is dependent upon the total pyrites liberated from the coal.

SEM microphotographs and EDAX scans of the cross section and outer surface of the slag deposit, illustrated in Figure 9, indicate the chemistry of the deposit is not uniform. The bulk of the fused material is rich in silica, low in iron, and virtually depleted of potassium. The outermost layers, no more than 2 to 3 μ thick, are very rich in iron and frequently also rich in calcium. On occasions, the outer surface is covered with small particulate several microns in diameter or undissolved cubic or octahedral crystals whose origin is pyrites. Similar formations have been observed in full-scale operation. The evidence indicates deposits form under axial symmetric flow conditions in the furnace by the fluxing action at the heat transfer surface of small particles, <8 μ in diameter, of decidedly different chemical composition and mineral source. Migration of the fly ash to the surface is by means of eddy diffusion, thermophoresis, or Brownian motion.

Sintered deposits form at the furnace exit at lower gas temperatures and in zones subject to rapid changes in direction. The deposit is composed of spheroidal particles <40 μ bound together by a molten substance. In those cases where substantial quantities of coarse pyrites are liberated from the pulverized coal, the spheroids are nearly pure Fe₂O₃, as shown in Figure 10. The matrix contained silica, alumina, iron, and potassium and has an initial deformation temperature of 1000°C, as determined by differential thermal analysis. The heavier pure iron spheroids deposit as a result of inertial impact. The mineral source of the molten phase is most likely illite.

Deposits also form on the leading edge of the first row of tubes in the convection pass when firing coals which liberate pure, coarse pyrites. These tubes are subjected to high gas velocities and have moderate to high collection efficiencies for particles between 40 and 100 μ . The deposits are nearly pure Fe₂O₃. They are hard and fused despite being at gas temperatures below their initial deformation temperature. No doubt, the final stages of decomposition of the pyrites takes place at the tube surface.

CONCLUSIONS

The formation of fireside deposits in furnaces depends on the composition, size, and association of mineral matter liberated from the coal. Selective deposition of specific mineral species depends on their size, thermal behavior, the local gas temperatures, and their mode of transport to the surface. Consequently, the composition of the sintered deposit or molten slag may vary with time at a given location and will most probably vary throughout the combustor, depending on local temperatures and fluidynamics. The composition of the slag may be substantially different from the composite coal ash, depending upon its heterogeneity. Illite is a likely candidate as the mineral most responsible for initiating deposits. The molten phases are frequently part of the FeO-SiO₂ or FeO-CaO-SiO₂ system and depend on the interaction of quartz, calcite, or pyrites at the heat transfer surface. Liberated pyrite crystals and small particles are primary candidates for slag formation subjected to parallel flow regimes at low velocities. Coarse pyrites can be selectively deposited and solely responsible for deposit formation on surfaces subjected to flue gas impingement at high velocities.

ACKNOWLEDGMENTS

Substantial portions of this study were sponsored by the U. S. Department of Energy, Pittsburgh Energy Technology Center, Contract DE-AC22-81PC40268, under the direction of Mr. J. Hickerson, Mr. H. Ritz, and Dr. R. Walker. I am grateful to Mr. O. R. Walchuk for supervising the combustion program; Mr. G. Lantos, who

directed laboratory analyses; Messrs. G. Stanko and I. Dojcsanszky for SEM and EDAX analyses; and Mrs. J. Betyeman for preparing the manuscript.

REFERENCES

1. R. W. Bryers, "The Physical and Chemical Characteristics of Pyrites and Their Influence on Fireside Problems in Steam Generators," Trans. of the ASME, Journal of Engineering for Power, October 1976.
2. F. E. Walker and E. F. Hartner, "Forms of Sulfur in U.S. Coals," IC830, Bu. Mines, U.S. Dept. of the Interior, 1966.
3. H. J. Gluskoter and J. A. Simon, "Sulfur in Illinois Coals," Circular 432, Illinois State Geological Survey, Urbana, Illinois, 1968.
4. P. Nicholls and W. A. Selvig, "Clinker Formation as Related to the Fusibility of Coal Ash," U.S. Bureau of Mines Bulletin 364, 1932.
5. J. F. Barkley, "The Sulfur Problem in Burning Coal," Technical Paper 436, Bu. of Mines, U.S. Dept. of the Interior, 1928.
6. "Sulfur Codes Pose Dilemma for Coal," Environmental Science and Technology, Vol. 11, No. 12, December 1970.
7. Hobart M. King and John J. Renton, "The Mode of Occurrence and Distribution of Sulfur in West Virginia Coals," Carboniferous Coal Guide Book, A. Donaldson, M. W. Presley, and J. J. Renton, Editors, West Virginia Geological and Economic Survey Bulletin B-37-1, 1929.
8. M. Deul, "Preliminary Observation of the Mode of Occurrence of Pyrite in Coal," Second Conference, Eastern American Anthraologist, University Park, Pennsylvania, May 26, 1958, p. 27.
9. Hobart M. King, "Sulfide Minerals in West Virginia Coals," Mountain State Geology, West Virginia Geological and Economic Survey, December 1980.
10. R. W. Bryers, "Influence of the Distribution of Mineral Matter in Coal on Fire-side Ash Deposition," Trans. of the ASME, Journal of Engineering for Power, October 1979.
11. R. C. Flagan and A. F. Sarofim, "Transformation of Mineral Matter in Coal," Progress in Energy and Combustion, to be published.
12. H. R. Hoy, A. G. Roberts, and D. M. Wilkins, "Behavior of Mineral Matter in Slagging Gasification Processes," I.G.E. Journal, June 1965.
13. P. Jackson, "From Mineral Matter to Deposits in PF-Fired Boilers, Part I: The Behavior of Mineral Matter in the Flame," Pulverized Coal Firing - The Effects of Mineral Matter, T. Wall, ed., University of Newcastle, August 1979.
14. J. D. Watt, "The Physical and Chemical Behavior of the Mineral Matter in Coal Under the Conditions Met in Combustion Plants: A Literature Survey--Part I: The Occurrence, Origin, Identity, Distribution, and Estimation of the Mineral Species in British Coals," BCURA Industrial Laboratories, Leatherhead, Surrey, England, August 1979.

15. N. W. Nelson, et al., "A Review of Available Information on Corrosion and Deposits in Coal- and Oil-Fired Boilers and Gas Turbines," ASME, 1954.
16. R. E. Honig, "Sublimation Studies of Silicon in the Mass Spectrometer," Journal of Chemistry and Physics, Vol. 77, 1954, pp. 1610-1611.
17. M. Th. Mackowsky, "The Behavior of Coal Minerals at High-Combustion Temperatures with Consideration of Slow and Rapid Heating," Paper Given at The Annual Meeting of the Association of Large Boiler Owners, Nürnberg, Germany, July 1955.
18. R. J. Quann and A. F. Sarofim, "Vaporization of Refractory Oxides During Pulverized Coal Combustion," Nineteenth Symposium International on Combustion, The Combustion Institute, 1982.

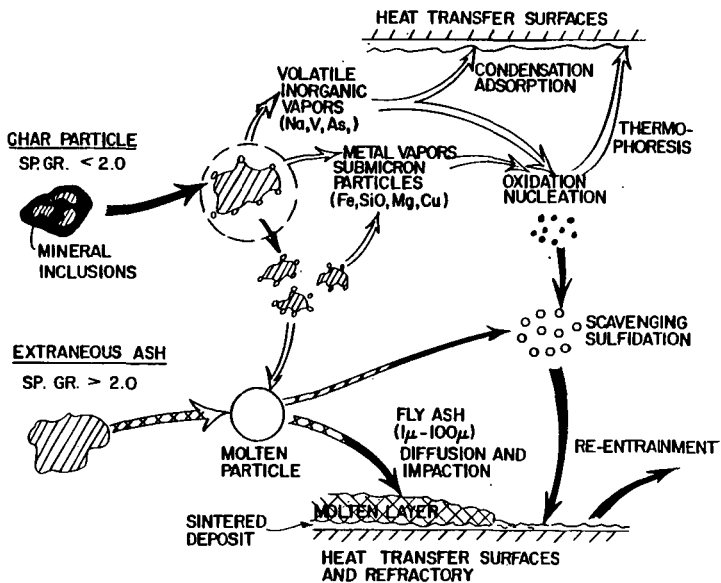


Figure 1 Fate of Mineral Matter in Coal During Combustion, as Proposed by Dr. Sarofim

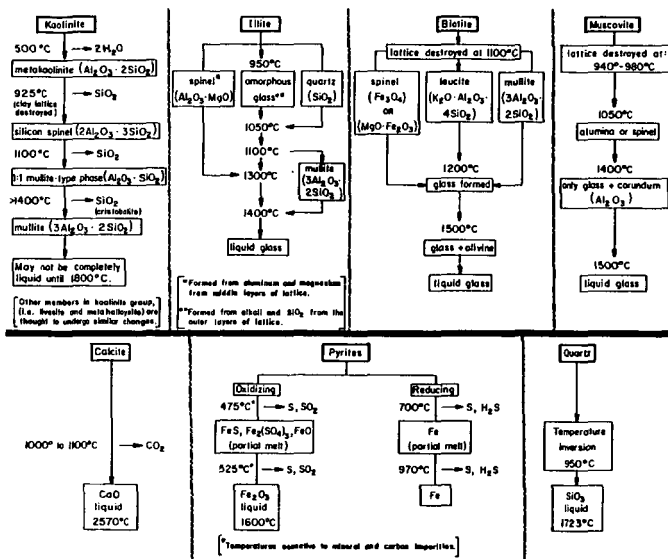


Figure 2 Phase Transformation of Some Mineral Matter Commonly Found in Coal

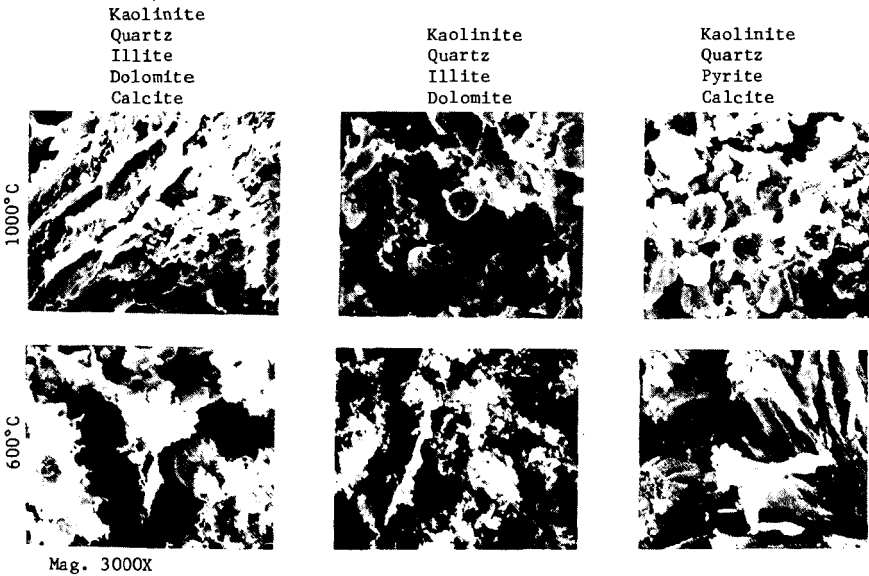


Figure 3 SEM Photomicrographs Showing the Impact of Illite on the Thermal Behavior of Low Temperature Ash

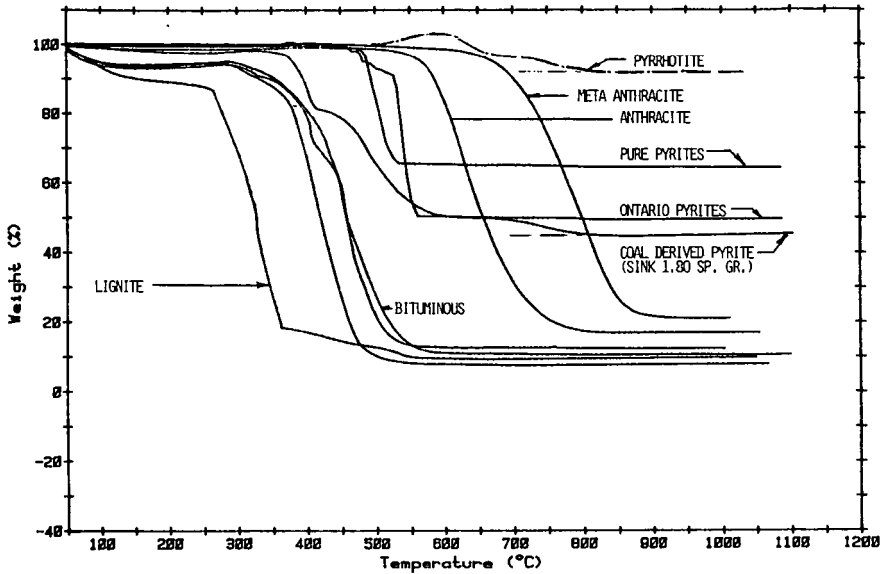


Figure 4 TGA Thermograms Comparing the Decomposition of Various Grades of Pyrites with Various Ranks of Coal

Mag. 3000X

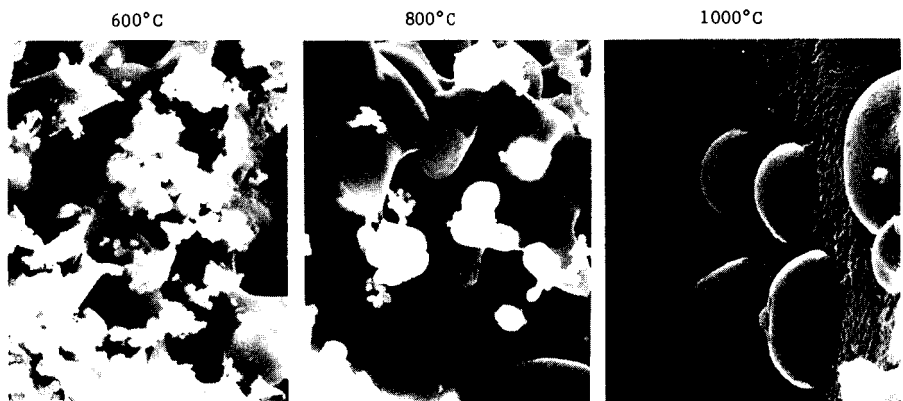


Figure 5 Pure Pyrites Heated Under Reducing Conditions to 600, 800, and 1000°C

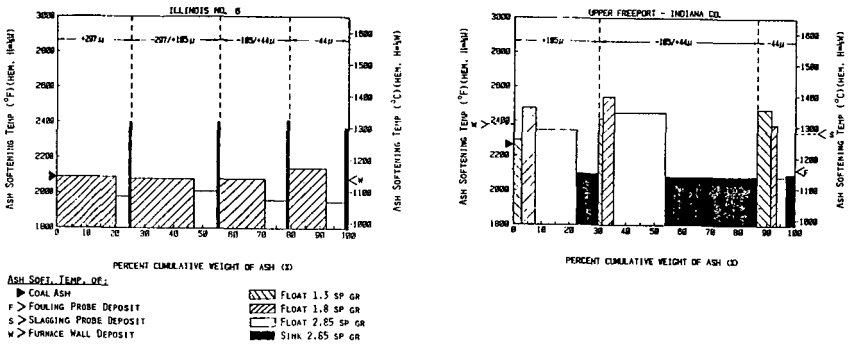


Figure 7 Fusibility Diagrams

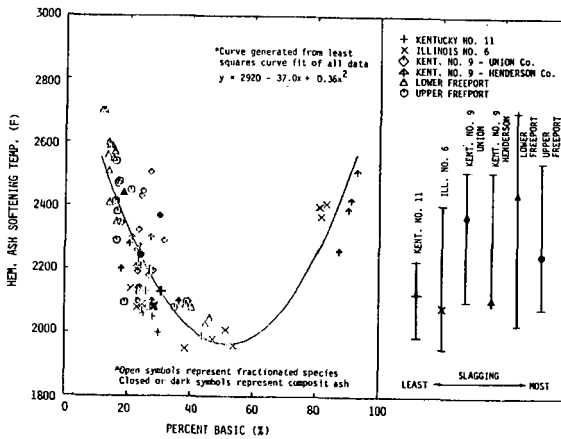


Figure 6 Ash Softening Temperature Vs. Percent Basic for Composite and Fractionated Coal Species

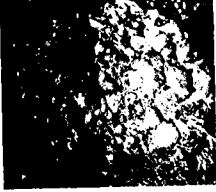
Ash Soften. Temp. (Red) and % Ash	% Liberated Fe_2O_3 in Coal	Probe	% Kin Ash	Ash Soften. Temp. (Red) and % Ash
2130°F 14.9	Kentucky No. 11 0.225		Western Fuel 1 0.2	2165°F 6.7
2080°F 9.4	Illinois No. 6 0.159		Western Fuel 2 1.0	2252°F 16.67
2443°F 16.4	Lower Freeport 1.56		Western Fuel 3 1.2	2232°F 25.73
2245°F 23.5	Upper Freeport 1.67		Lower Freeport 2.5	2443°F 16.4

Figure 8 Slagging on Furnace Probes after 14 - 16 Hours Operations

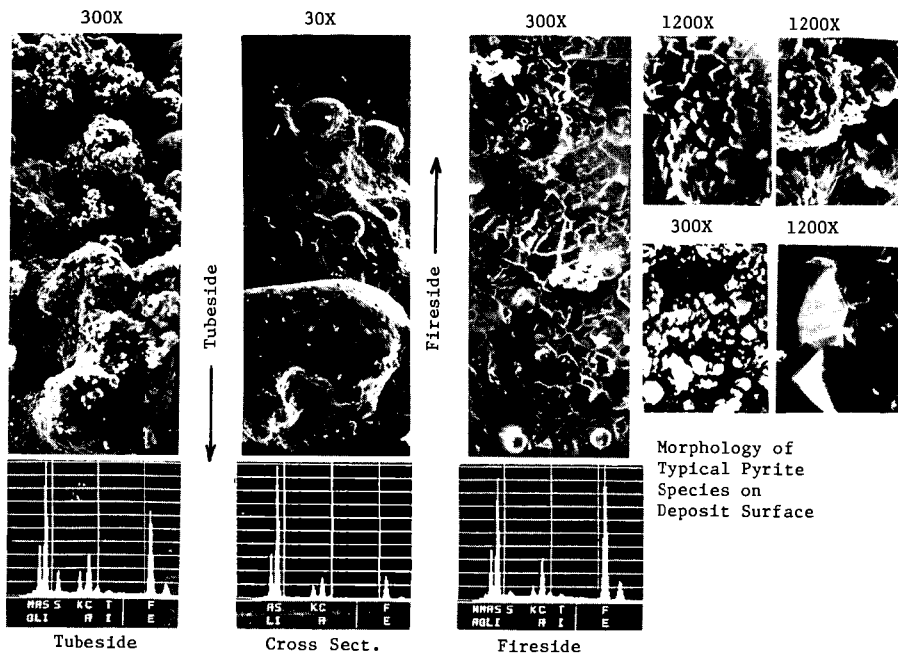


Figure 9 Slag Formation on Furnace Slag Probe

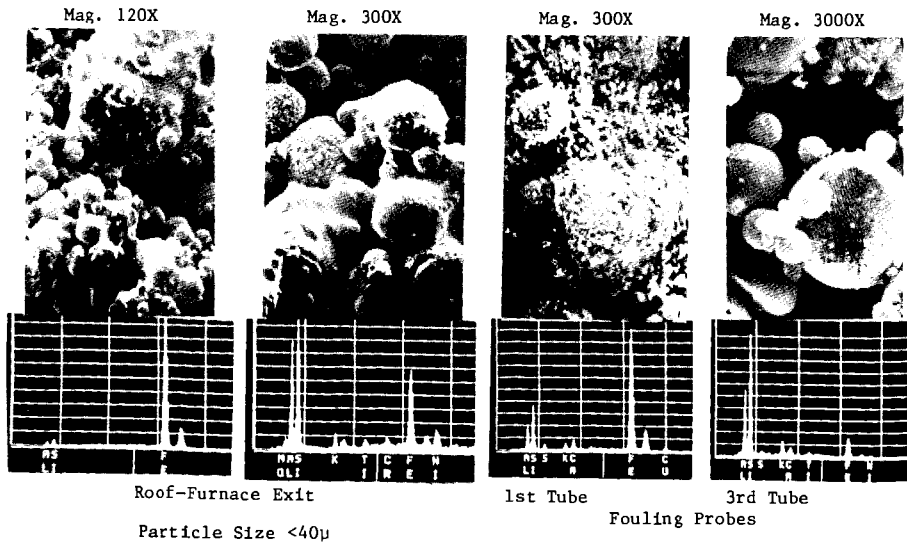


Figure 10 Iron-Rich Sintered Deposits Formed on Furnace Roof and 1st Tube of Convection Pass Probes by Coarse Pyrites

INFLUENCE OF THERMAL PROPERTIES OF WALL DEPOSITS ON PERFORMANCE OF P.F. FIRED BOILER COMBUSTION CHAMBERS

W. Richter, R. Payne, and M.P. Heap

Energy and Environmental Research Corporation
Irvine, CA 92714

1.0 INTRODUCTION

The build-up of ash deposit layers on tube walls and superheaters in dry bottom p.f. boiler combustion chambers not only deteriorates furnace and overall boiler efficiency; but increases the temperature level in furnace and convective passages and aggravates existing deposit problems. This can finally lead to expensive outages when deposit formation cannot be controlled by soot blowing alone. Since errors in furnace design with respect to slagging and fouling or wrong estimation of impact of fuel conversion on deposit formation are so costly in large boilers, there is considerable financial incentive to develop analytical methods in order to predict furnace performance for a wide range of coal types and operating conditions. It is clear that such methods must take quantitatively into account, among other things, the thermal properties of ash deposits.

The properties which determine heat transfer through a deposit layer of given thickness are thermal conductivity, emissivity, and absorptivity. The current paper presents results from various studies carried out by the authors at Energy and Environmental Research Corporation (EER) to show the sensitivity of overall furnace performance, local temperature and heat flux distributions on the properties of deposits in large p.f. fired furnaces.

2.0 PARAMETRIC STUDY OF OVERALL FURNACE PERFORMANCE

The most important parameters for overall furnace heat absorption are the adiabatic flame temperature, the firing density per heat sink area, the emissivity of the furnace volume, temperature and emissivity of the heat sinks and the flow and heat release patterns. Figure 1 shows how these quantities are related in a complex manner to each other, to fuel characteristics and to operating and boundary conditions of the furnace. Some of the relationships of Figure 1 were approximately quantified utilizing a simple well-stirred furnace model (1) which assumed transport of grey radiation. Two important results for furnace performance with respect to formation of deposits are shown in Figures 2 and 3, in which furnace efficiencies η_f ,

$$\eta_f \equiv 1 - \frac{\dot{M}_0 c_p \int_{T_0}^{T_{ex}} (T_{ex} - T_0)}{\dot{Q}_0} \quad (1)$$

are plotted over furnace height L with surface temperatures T_w of deposits and surface emissivities ϵ_w as parameters. The calculations were carried out for a rectangular furnace box of width $L/3$. Other input parameters are

listed in the Figures. The grey absorption coefficient K_a of 0.1 1/m used in the examples corresponds to an emissivity $\epsilon_f = 0.55$ for a furnace volume with a height of $L = 30\text{m}$. The effect of deposit surface temperature T_w on furnace efficiency η_f is considerable for values larger than 700 K (Fig. 2). For instance a furnace efficiency of 0.40 (corresponding to $T_{ex} = 1440\text{ K}$ according to Equation 1) was obtained for $T_w = 700\text{ K}$ (see Section 3 and 4). The L must be increased by 16.5m or 53% of the original height with clean walls to achieve the same furnace efficiency for a furnace with wall deposit of surface temperature 1300 K.* The impact of wall temperature on η_f will be even stronger for adiabatic flame temperatures less than 2200 K. Such adiabatic flame temperatures can occur when firing lignite or high-moisture coals. For furnaces operated with the same thermal input at low efficiencies, the presence of wall deposits requires only a moderate increase in size.

A reduction of surface emissivities from 1 (clean "sooty" walls) to 0.4 (which is the lowest range reported for ash deposits (see Section 3) also causes a drop of η_f (Fig. 2). However, the required increase in size to maintain η_f is smaller than for the change of deposit surface temperatures from 700 K to 1300 K mentioned above. The size changes non-linearly with changes of surface temperature but nearly linearly with ϵ_w between $\epsilon_w = 1$ and $\epsilon_w = 0.5$. Beyond $\epsilon_w = 0.2$, L must increase non-linearly to maintain furnace efficiency.

When a deposit layer is formed, surface temperature is increased and wall emissivity decreased. However, the superposition of these effects on η_f is less than a pure summation; since, by decreasing ϵ_w , the net heat flux to the layer is reduced, thus retarding the increase of surface temperature to a certain extent.

3.0 AVAILABLE DATA OF THERMAL PROPERTIES OF ASH DEPOSITS AND DATA ANALYSIS

Thermal Conductivity. A comprehensive review of literature data for thermal conductivity k of ash deposits was published by Wall et al. (2). The thermal conductance, k , of the ash material increases reversibly with temperature until sintering or fusion occurs. At this stage, a rapid and irreversible increase of k is observed. Typical values of k for non-sintered deposits from Australian coals in actual furnaces vary between $0.1 \cdot 10^{-3}\text{ KW/mK}$ at 500 K up to $0.4 \cdot 10^{-3}\text{ KW/mK}$ at 1300 K. The factors contributing to the thermal conductance in the powdered deposits are: Conductance in the solid particles, gas conduction in the voids and radiative transfer through the voids. Fetters et al. recently measured k for boiler deposits of an Indiana coal (3) and point out that the dominant mode of heat transfer through the deposit layer is by radiation at high temperature. The values of k measured for powdery deposits by Fetters et al. are about 2 times larger than those of

* 1m of furnace height corresponds to $\approx 500,000\text{\$}$.

Wall et al. (2) at the same temperature. This is contributed to the relative large particle sizes of the Indiana coal ash (75% in the 100 μ m range) compared to the Australian coal ash with mean weight particle diameters of 50 μ m and less.

Thermal conductivity of sintered and fused deposits found by the Australian researchers range from 0.5 10^{-3} KW/mK at 800 K to 1.2 10^{-3} KW/mK at 1500 K. This is consistent with the recent findings of Fetters et al. (3) for crushed deposits from a boiler fired with Indiana coal and other literature values (4). The increase of thermal conductivity of sintered and fused deposits is due to a decrease of void space and increased transmissivity of the material. Assuming uniform mean conductivity, the thickness of a sintered deposit layer which maintains fusion at its surface can be estimated by

$$\Delta s_{fu} = \frac{k (T_{fu} - T_{t,a})}{\epsilon_w q_{in} - \epsilon_w \sigma T_{fu}^4} \quad 2)$$

where T_{fu} is the ash fusion temperature, $T_{t,a}$ the temperature of the outer surface of the tubes and q_{in} the incident heat flux density. With typical values $k = 0.8 \cdot 10^{-3}$ KW/mK, $T_{fu} = 1550$ K, $\epsilon_w = 0.7$, $T_{t,a} = 750$ K and $q_{in} = 400$ KW/m² the layer thickness with a wet surface would be about 8 mm. Wall et al. emphasize that values of k obtained from ground deposits in laboratory studies are questionable since bounding of the deposit occurs in situ which leads to an increase of k . This agrees with our results for a 700 MW_e boiler which yielded an overall value of $k = 3.2$ KW/m²K for deposits which could not be removed by soot blowing (see Section 4).

Emissivity and Absorptivity

Reviews of emissivity data of ash deposits were given by Wall et al. (2) and recently by Becker (5). The literature data has a considerable spread of emissivity, between values of $\epsilon_w = 0.9$ and $\epsilon_w = 0.3$ depending on temperatures, ash origin and probe preparation. However, general agreement exists that, for non-sintered material ϵ_w decreases reversibly with surface temperature. After sintering, the emissivity changes irreversibly to higher values (2). This agrees with measurements of furnace generated deposits of American coals carried out by Goetz et al. (6). These authors report values between 0.38 and 0.67 for powdery (initial) deposits, values between 0.76 and 0.93 for sintered deposits and values 0.65 and 0.85 for glassy and or molten deposits. The increase of emissivity with sintering and fusion is due to increased transmission of radiation into the surface of the deposit layer. In the range of surface temperatures of interest, namely between 800 K and 1400 K, measured total emissivities on probes of sintered real furnace deposits exhibit only slight variations with surface temperature (5), (6). However, measurements by Becker of spectral emissivities of deposits on laboratory prepared probes showed distinctive non-grey behavior. For typical flame temperatures of 1700 K and typical surface temperatures of 1100 K, up to 0.2 higher values were found for emissivities than for absorptivities. Non-greyness of emission and absorption is typical for glassy material and is due to the low spectral absorptivities at short wavelengths which becomes dominant for radiative transfer at more elevated flame

temperatures. The assumption of grey radiation of furnace deposits and consequent use of grey emissivity values for determination of absorption may lead to errors in heat transfer calculations for furnaces with moderate deposits since at lower surface temperatures absorption is several times larger than re-emission. By performing detailed one-dimensional spectral calculations, Becker showed that for a 10 m path length, typical of furnaces, and relatively cool walls errors up to +30% in predicted net heat flux densities would result from the assumption that the deposits were grey. However, these findings are based on spectral values found for laboratory prepared probes. Spectral measurements of real furnace deposits show reduced non-grey behavior (5), (6) and higher emissivities than the laboratory probes (6). Moreover, coloring agents such as unburnt carbon as well as the rough surface structure of real deposits and tube curvatures tend to make boiler surfaces more closely approximate grey behavior. Thus, the importance of non-grey deposits is uncertain in boiler chambers and, in any case, insufficient information is available to recommend replacing the assumption of grey radiation of deposits currently used in 3-D furnace models (see Section 4) by expensive more rigorous spectral models.

4.0 PREDICTIONS OF INFLUENCE OF WALL DEPOSITS ON HEAT TRANSFER IN EXISTING BOILERS

On the basis on the literature values of thermal properties discussed above a considerable number of performance predictions have been carried out for existing boiler combustion chambers in the past two years. Some results of those calculations with relevance to the impact of ash deposits on heat transfer follow. The tool used for the analysis is an extreme flexible 3-D Monte-Carlo type zone model (7), (8). In this model, the emissive power of each volume and surface zone is distributed into a discrete number of radiative beams. Taking multiple reflection at furnace walls into account, the beams are traced throughout the furnace volume until final absorption. Non-greyness of the combustion products is modeled with a weighted grey gas approach. The radiating species considered are H₂O, CO₂ and particulates (soot, char and ash). Currently, char and ash particles are treated as grey radiators. The model of radiative exchange is directly coupled with a total heat balance of volume and surface (deposit) zones with unknown temperatures. The calculation of convective heat fluxes through the furnace is based on mass flow vectors at the boundary of each zone obtained from isothermal modeling. The heat release pattern is based on this flow field. The heat release due to volatile combustion is based on observed visible flame length and the heat release due to burnout of char particles is calculated from carbon and oxygen balances solved simultaneously with the heat balance.

Example 1: Tangentially Coal-Fired Boiler

This study was carried out to investigate the influence of ash deposits in a twin furnace of a boiler originally designed to fire No. 6 oil at a net thermal input of 1000 MW_t. However, the thermal input of the furnace was reduced to 590 MW_t to investigate the prospects of firing coal in this unit. The coal considered was a Utah coal with 8.8% ash content fired with 30% excess air. Figure 4 shows the zoning of the furnace and the assumed flow

patterns. The heat release due to combustion is indicated by the shaded area. The surface conditions were specified by the following input data:

- Case A Clean surfaces, emissivity of tubes $\epsilon_w = 0.9$
- Case B Powdery ash deposit, $\epsilon_w = 0.6$, $\Delta s = 0.5\text{mm}$, $k = 0.3 \cdot 10^{-3} \text{ KW/mK}$
- Case C Properties of ash deposit layer in upper part of the furnace (above heat-release zone) as specified for Case B; glassy ash deposit layer in lower part of the furnace with $\epsilon_t = 0.8$, $\Delta s = 7\text{mm}$, $K = 1 \cdot 10^{-3} \text{ KW/mK}$.

The properties for the powdery (primary) and for the glassy (molten) deposit layer of the Cases B and C correspond to average data from literature as cited above. The actual calculations were carried out with an effective emissivity of the tube walls taking the shadow effect of the gap between adjacent tubes into account.

Table 1 and Figures 5 through 7 show that the build-up of ash deposits seriously affects overall and local heat transfer. The difference ($\Delta\eta_f$) in computed furnace efficiencies for the extreme cases, A (clean walls) and C (highest thermal resistance), is 6.2 percentage points. The formation of a first initial deposit layer (Case B) has a stronger impact on heat transfer than subsequent increase of deposits in the lower furnace (Case C). The increase of the thickness of ash deposit opposite to the heat release zone displaces the peak heat fluxes up into the regions of the thinner deposits (Fig. 6). This is one reason why the build up of deposit layers, once started, spreads into adjacent wall zones. Once the deposit layers begin growing, surface temperatures can soon reach values in the range between softening (1400 K) and fusion temperature (1500 K) as indicated by shaded areas in Fig. 7. The furnace model is also able to predict, for a given coal ash fusion temperature approximately the development and extent of molten slag layers.

Another investigation showed for the same boiler fired with COM at a rate of 875 MW_t , showed that a decrease of surface emissivity from 0.9 (clean) to 0.6 (initial deposit) raised mean furnace exit temperature by 55 K.

Example 2 Opposed P.F. Fired Boiler

This study was carried out in order to verify the 3-D furnace heat transfer model with performance data available from a coal-fired, boiler combustion chamber of 1732 MW_t fuel heat input. The coal had a medium volatile content, an ash content of 6.6%, and was fired with 28% excess air. In this case, the flow pattern was based on detailed distribution of mass mean flow vectors measured in a physical isothermal model. However, turbulent components were superimposed on these vectors with the help of a simple model of turbulence. Fig. 8 shows a comparison of the profiles of gas temperatures measured and predicted for 100% Load in one half of the furnace outlet plane. The difference between predicted and measured values was less than 25 K. The good agreement is partially due to a reasonable assumption of the effective heat conduction coefficient $(k/\Delta s)_{\text{eff}}$ of the deposit layers. Fig. 9 shows how the predicted mean furnace exit temperature varied with $(k/\Delta s)$

s)eff and compares those predictions with two data points obtained from measured heat balances of the boiler immediately after soot blowing and 20 h after soot blowing. Since measurements and observations yielded approximately a 2mm deposit layer, which could not be removed by soot blowing an effective thermal conductivity of $3.2 \cdot 10^{-3}$ /mK can be deduced. An assumed value of $k = 0.8 \cdot 10^{-3}$ KW/mK for a dry partially sintered deposit would suggest the build-up of an additional layer of 1.5 mm, 20 h after soot blowing for a total layer of 3.5 mm thickness.

Fig. 9 also contains the relationship of $T_{ex} = f(k/\Delta s)$ for a similar boiler of 1250 MW_t heat input in which slagging and fouling problems are encountered. Further applications of the 3-D furnace model with respect to impact of wall deposits on heat transfer in CWM and COM fired furnaces may be found in (5), (10).

5.0 CONCLUSIONS

Thermal conductivity and emissivity of wall deposits have a considerable effect on heat transfer in large boilers. This results in temperature differences of furnace exit temperatures which influence furnace height, performance and costs. More exact values of deposit thermal properties, which vary over a wide range of temperatures and conditions, than currently available are needed for detailed prediction of the initial formation of deposit layers. However, gross characteristics of thermal properties can be assumed and are sufficient to estimate the performance of furnaces, since the model contains other major uncertainties such as, thickness and inhomogenous distribution of deposits at furnace walls and superheaters. This is especially true between soot blowing cycles. The 3-D heat-transfer model used in the present study has the potential to form the basis of a more comprehensive model of slagging and fouling because it can provide reliable predictions of flame and deposit temperatures. A model of ash transport is currently being coupled with the furnace heat transfer model which will account for time-temperature histories of ash and wall collisions.

6.0 LITERATURE

- (1) Richter, W.: Parametric Screening Studies for the Calculation of Heat Transfer in Combustion Chambers. Topical Report, prepared for Pittsburgh Energy Technology Center, Department of Energy, under Contract No. DE-AC22-80PC30297, January 1982.
- (2) Wall, T. F., A. Lowe, L. J. Wibberley, and McC. Stewart: Mineral Matter in Coal and the Thermal Performance of Large Boilers. Prog. Energy Combust., Science, Vol. 5, pp. 129, 1979.
- (3) Feters, G. D., R. Viskanta, and F. P. Incropera: Experimental Study of Heat Transfer Through Coal Ash Deposits. 1982 ASME Winter Annual Meeting, Paper 82-WA/HT-30.
- (4) Singer, J. G., Editor: Combustion: Fossil Power Systems, 3rd Edition, Combustion Engineering Inc., Windsor, p. C-16, 1981.

- (5) Becker, H. B. : Spectral Band Emissivities of Ash Deposits and Radiative Heat Transfer in Pulverised-Coal-Fired Furnaces. Ph.D. Thesis, University of Newcastle, Australia, February 1982.
- (6) Goetz, G. J., N. Y. Nsakala, and R. W. Borio: Development of Method for Determining Emissivities and Absorptivities of Coal Ash Deposits. Journal of Engineering for Power, Vol. 101, pp. 607-619, 1979.
- (7) Richter, W., and M. P. Heap: A Semistochastic Method for the Prediction of Radiative Heat Transfer in Combustion Chambers. Western States Section, The Combustion Institute, 1981 Spring Meeting, Paper 81-17, 1981.
- (8) Richter, W., and M. P. Heap: The Impact of Heat Release Pattern and Fuel Properties on Heat Transfer in Boilers, 1981 ASME Winter Annual Meeting, Paper 81 WA/HT27, 1981.
- (9) England, G. C., Y. Kwan, W. Richter and K. Fujimura: Studies to Evaluate the Impact of Conversion from Fuel-Oil to Coal-Oil Mixtures on Thermal Performance and Pollutant Emissions. Pittsburgh Energy Technology Center, Proc. of the Fourth International Symposium on Coal Slurry Combustion, Vol. 3, 1982.
- (10) Payne, R., S. L. Chen and W. Richter: A Procedure for the Evaluation of the Combustion Performance of Coal-Water Slurries. Fifth International Symposium on Coal Slurry Combustion and Technology, Session VII, DOE, PETC, 1983.

Table 1. Thermal Performance of 590 MW_t Coal-Fired Combustion Chamber For Various Slagging And Fouling Conditions

No.	Case	Furnace Efficiency	Mean Furnace Exit Temperature	Mean Net Heat Flux Density	Max. Net Heat Flux Density	Vertical Position of Max. Net Heat Flux Density	Max. Flame Temp.	Max. Furnace Exit Temp.	Unburnt Cfix	Carbon Content of Fly Ash
		%	K	KW/m ²	KW/m ²	m	K	K	%	%
A	Clean Surfaces	40.3	1436	168	304	14.9	1661	1515	1.35	6.43
B	Powdery Ash Deposit	35.6	1519	148	235	16.7	1728	1582	0.89	4.33
C	Slagging Lower Half	34.1	1541	143	239	19.2	1776	1610	0.75	3.68

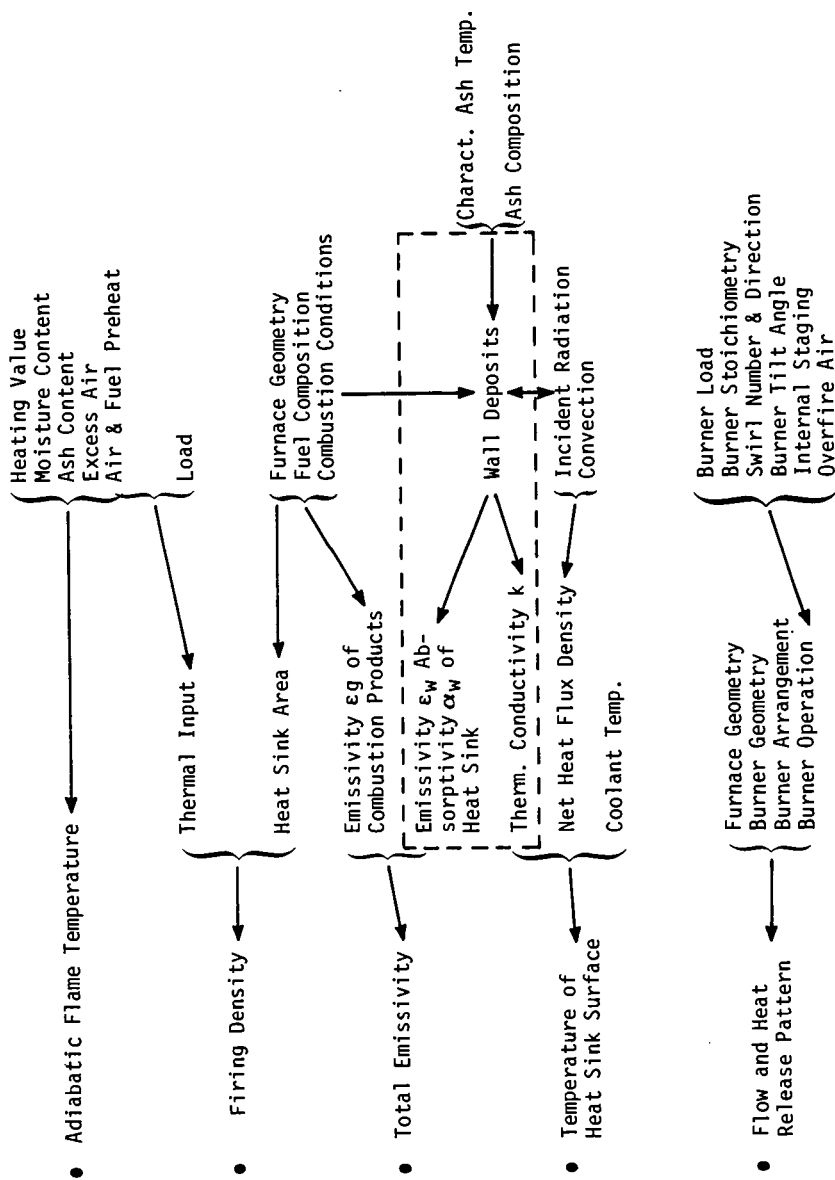


Figure 1. Major Factors Influencing Thermal Performance of Furnaces

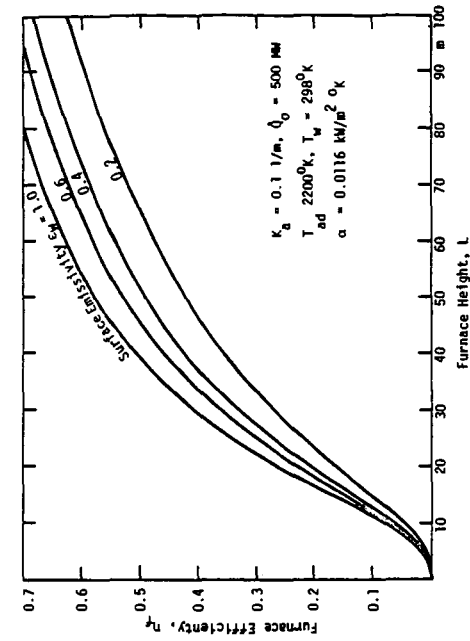


Figure 3. Dependency of Furnace Efficiency on Furnace Height With Surface Emissivity as Parameter.

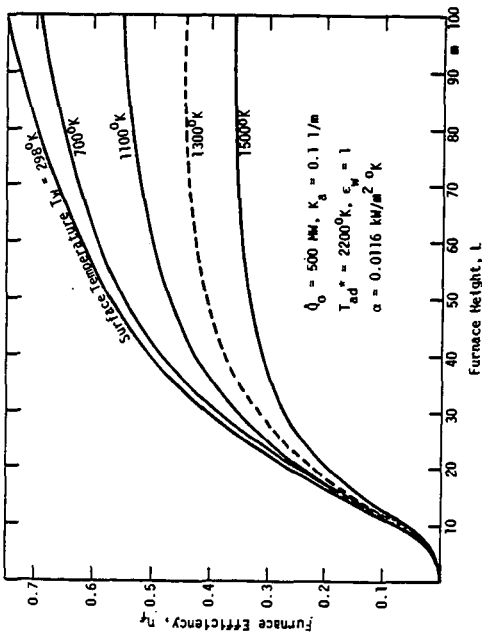


Figure 2. Dependency of Furnace Efficiency on Furnace Dimensions for Various Surface Temperatures.

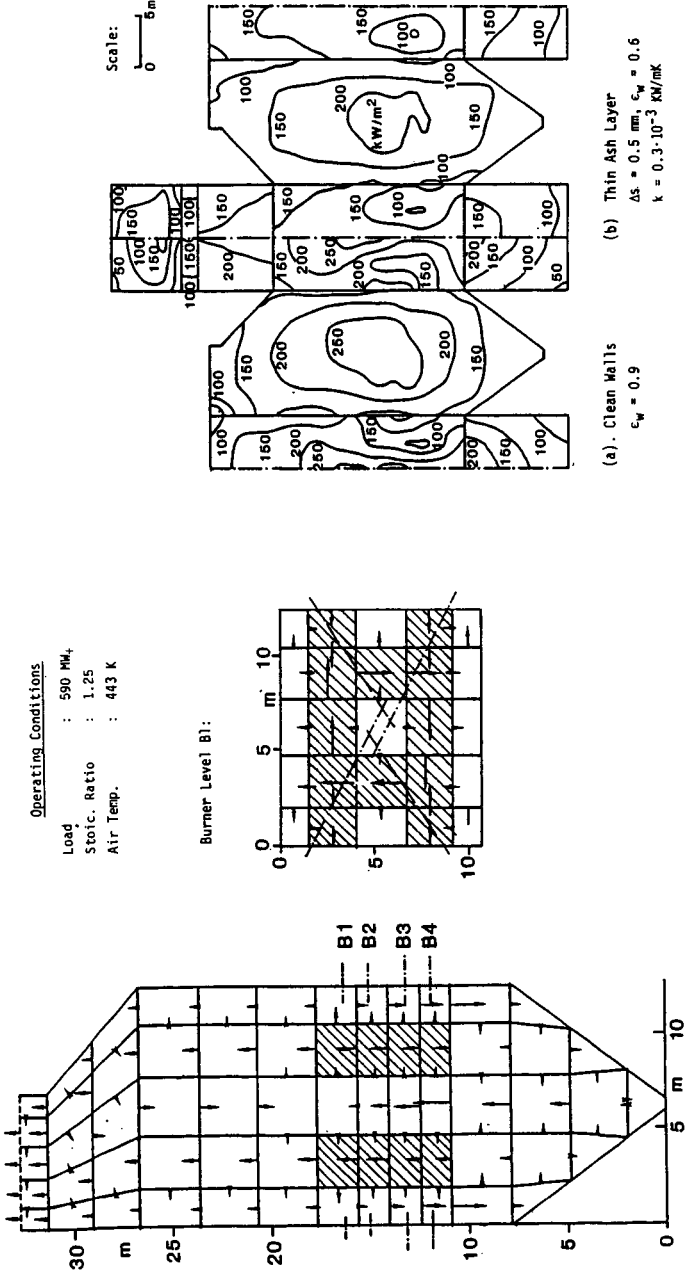


Figure 4. Geometry and Zoning of Tangentially Fired Boiler Originally Designed for Oil Firing with 1000 MW_t Thermal Input.

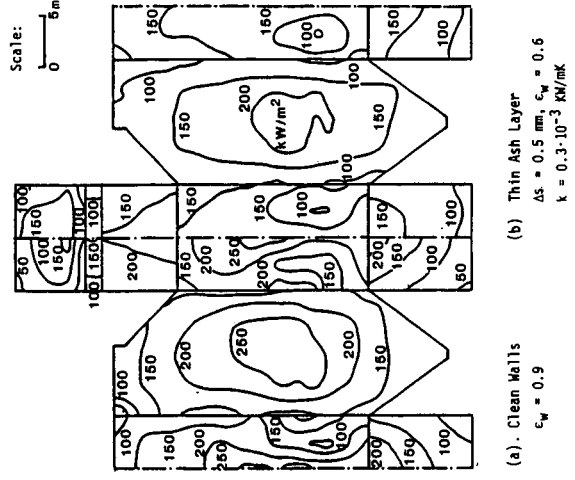


Figure 5. Influence of Wall Deposits on Predicted Net Heat Flux Distribution in Boiler Combustion Chamber Fired with Coal at a Rate of 590 MW_t.

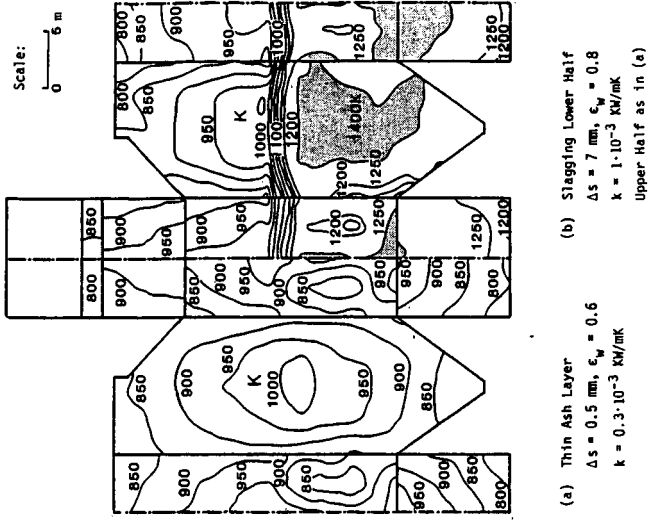


Figure 7. Influence of Slagging in Lower Furnace Half on Predicted Surface Temperatures of Deposits in Boiler Combustion Chamber Fired with Coal at a Rate of 590 MWt.

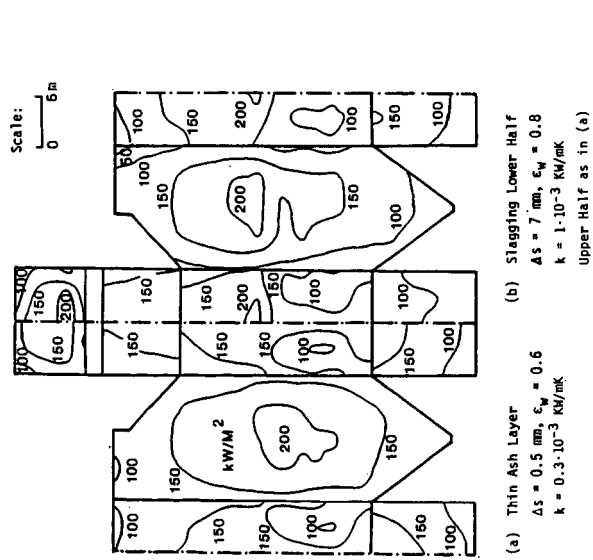


Figure 6. Influence of Slagging in Lower Furnace Half on Predicted Net Heat Flux Distribution in Boiler Combustion Chamber Fired with Coal at a Rate of 590 MWt.

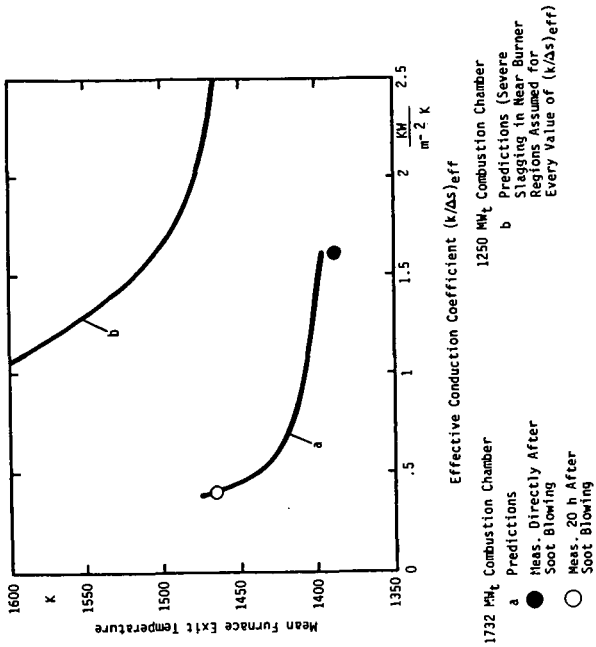


Figure 9. Dependence of Mean Furnace Exit Temperature on Effective Conduction Coefficient for Two Opposed Coal-Fired Boiler Combustion Chambers.

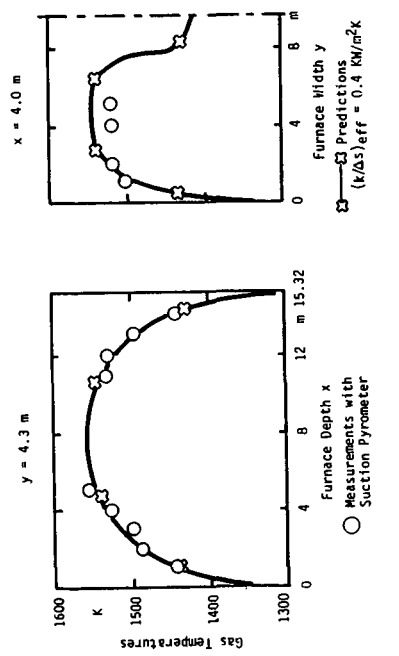


Figure 8. Comparison of Temperature Profiles Predicted and Measured Near Furnace Exit ($z = 68.6 \text{ m}$) of 1730 MW_t Opposed Coal-Fired Boiler Combustion Chamber.

The Prediction of the Tendency of Slagging and
Fouling of European Lignites by New Statistical
and Experimental Methods

W. Altmann
Technical University of Dresden
Mommenstrasse 13
8027 Dresden

German Democratic Republic

Communicated by:

John H. Pohl
Energy and Environmental Research Corporation
18 Mason
Irvine, California 92714

Introduction

Proper design and operation of coal-fired boilers requires prediction of the tendency of the fuels to foul and slag. A large number of correlations based on the oxides of an ash produced in the laboratory exist (1,2). The success of these correlations has been limited to the range of ash properties for which they were developed, and even then, these relationships may be unreliable. For instance, existing correlations can predict whether a fuel will create deposition problems in boilers rarely, occasionally, or frequently for approximately 50 percent of the fuels. An accuracy only slightly better than random guess (3).

Potential problems using available techniques have been discussed in the literature (2,3,4,5). The problems result from:

- Preparation and analysis of the ash (6)
- Ignoring the distribution and individual nature of mineral matter (4,6)
- Neglecting the influence of ash content (7)
- Ignoring the design of the boilers including heat release rate, heat fluxes and velocity profiles (3,8,9)

In addition the correlation should not be used for coals with properties outside the range for which the correlations were developed.

This paper describes the limited success of applying such techniques to predict performance, efforts to develop and verify new techniques to predict performance, and application of these techniques to predict the slagging and fouling behavior of European brown coals.

Prediction of Slagging Performance

Slagging performance of coals in boilers has been predicted by:

- temperature of critical viscosity,
- the base to acid ratio,
- and the base to acid ratio multiplied by the sulfur content of the coal.

Predictions of slagging and fouling using these relationships are compared to boiler performance for the six European brown coals listed in Table 1. The calculated indices and estimated and actual performance of the fuels are shown in Table 2.

The temperature of critical viscosity is the temperature at which the slag changes from plastic to Newtonian behavior. Plastic slags are difficult to remove by soot blowing. As a consequence, fuels with low temperatures of critical vis-

cosity are expected to form difficult to remove plastic and molten slags more readily than other fuels.

The temperature at critical viscosity can be measured in a viscometer, but the measurements are time consuming and expensive and the temperature at critical viscosity is usually estimated using empirical formulae. For instance, Watt and Fereday (10) developed

$$T_{CV} = \sqrt{\frac{107 \cdot m}{2.398 - c}} + 150 \text{ in } ^\circ\text{C} \quad 1).$$

$$\text{where } \text{SiO}_2 + \text{Al}_2\text{O}_3 + \text{Fe}_2\text{O}_3 + \text{CaO} + \text{MgO} = 1 \quad 2).$$

$$\text{and } m = 0.835 \text{ SiO}_2 + 0.601 \text{ Al}_2\text{O}_3 - 0.109 \quad 3).$$

$$c = 4.15 \text{ SiO}_2 + 1.92 \text{ Al}_2\text{O}_3 \quad 4).$$

The temperature at critical viscosity probably does not adequately predict slagging behavior of the six European brown coals of this study. The qualitative relationship between deposits formed in a boiler and the temperature of critical viscosity estimated by the technique of Watt and Fereday (10) is shown in Figure 1a. The data appear to correlate with observations, but predict improved performance at an intermediate temperature of critical viscosity. No reason is known for this and the correlation may be fortuitous.

The base to acid ratio is the reverse of the previous relationship and probably does not correlate the slagging data either. Figure 1b shows that the base to acid ratio appears to correlate the prediction of performance of brown coals in boilers. This relationship predicts optimum performance at a base to acid ratio of 0.3. This is quite possible with the formation of eutectics. However, comparison of Figure 1a and 1b shows the curves are reversed and the prediction of performance of all the fuels fall in the same relative position on both curves. This again leads to uncertainty as to the reasonableness and the reliability of the correlations in Figure 1.

The standard slagging factor, R_S , could not correlate the performance of all the fuels in the boilers. The slagging factor is defined as

$$R_S = B/A \cdot S \quad 5).$$

by Attig and Duzy (11). This equation is suggested for ashes which have $\text{Fe}_2\text{O}_3 > \text{CaO} + \text{MgO}$ but is applied to all ashes in this study. Only two of the ashes in this study have $\text{Fe}_2\text{O}_3 > \text{CaO} + \text{MgO}$. Leipzig has about equal amounts and Nordbohmen has greater Fe_2O_3 than $\text{CaO} + \text{MgO}$. The base to acid ratio (shown in Figure 2a) is recommended to correlate slagging behavior of ashes with $\text{CaO} + \text{MgO} > \text{Fe}_2\text{O}_3$ (11). Five of the fuels correlate reasonably with R_S but the slagging of Nordbohmen was greatly underestimated. However, this fuel was the only one with significantly greater Fe_2O_3 than $\text{CaO} + \text{MgO}$ and might not correlate with the other five fuels.

A good correlation of all six fuels was developed by modifying the slagging factor. The relationship is shown in Figure 2b where the slagging factor, f_S , is defined as:

$$f_S = 1.7 + 1.7 \text{ SiO}_2^* + 0.8 \text{ Al}_2\text{O}_3^* - 6.0 (\text{S})_{\text{Fe}}^0 \cdot 2 - 2.2 (\text{CaO}^* + \text{MgO}^*) - 1.95 \text{ SO}_3^* - 1.3 (\text{Alk})^* \quad 6).$$

where $f_S = 0$ is strong slagging

and $f_S = 1$ is no slagging

$$\text{and } [\]^* = \frac{[\]^*}{1 - \text{SiO}_2 + \text{SiO}_{2\text{corr}}} \quad (7).$$

$$\text{SiO}_{2\text{corr}} = 823 \Gamma_{\text{SO}_3}^{2.65} \cdot \exp(-9.45 \Gamma_{\text{SO}_3}) \text{Fe}_2\text{O}_3 \quad (8).$$

$$\Gamma_{\text{SO}_3} = \frac{\text{SO}_3}{1 - \text{SiO}_2} \quad (9).$$

where S is the weight percent sulfur in the coal as received and all other compositions are weight percent of the ash.

Predictions of Fouling Performance

The fouling performance of the six brown coals of this study could not be adequately predicted by existing or new techniques. The fouling performance of coals with $\text{CaO} + \text{MgO} > \text{Fe}_2\text{O}_3$ is usually predicted by the sodium content of the ash. Figure 3a shows the correlation of the qualitative observation of fouling in boilers with the alkali (Na_2O plus K_2O) content of the ash. All the coals except Ungarn correlate with the alkali content of the ash. However, no explanation is available for the fouling of the Ungarn which had 0.0 alkali content in the ash. A new fouling factor, f_F ,

$$f_F = \exp \left[\frac{-5. \text{Alk}^*}{\Gamma_S + 0.3} \right]$$

where Alk^* is defined by equation (7) was moderately successful, Figure 3b, in correlating the fouling performance of coals. However, considerable scatter still exists in the relationship.

Pilot Scale Prediction of Fouling and Slagging Performance

The limited success of predicting fouling and slagging performance based upon the analysis of the oxides of ashes produced in laboratory apparatus has prompted the Technical University of Dresden to develop pilot scale tests to predict slagging and fouling of ashes in boilers. Two tests are currently being evaluated which determine slagging and fouling characteristics of fuels not determined by current laboratory or other small scale tests. The first, determines the fouling and slagging of the fuel under different combustion conditions. In this test, the coal is burned in a small drop tube furnace. The level of oxygen and the thermal environment of combustion are changed. The particle temperatures are measured with thermographic techniques and the nature and deposition rate evaluated. Such a technique can simulate the limits of the time temperature concentration history in boilers and avoids production of an artificial mean ash. This technique does not account for ash trajectories in boilers.

The tendency of ash to follow streamlines or deposit on surfaces is determined in a second test. In this test, the coal is burned in a small cyclone combustion chamber. This chamber can also simulate the limits of time and temperature history of ashes in boilers. In addition, a cyclone chamber subjects the coal to centrifugal forces, which allows the ability of the fly ash particles to follow streamlines to be assessed.

The ability of these pilot scaled tests to predict the slagging and fouling performance of European brown coals is currently being evaluated. Preliminary results are promising.

TABLE I ASH COMPOSITION OF EUROPEAN BROWN COALS
WEIGHT PERCENT IN THE ASH

	UNGARN	LEIPZIG	NIEDERLAUSITZ	OBERLAUSITZ	NORDBOHMEN	SALZKOHLE
SiO ₂	47.9	25.5	46.2	41.8	52.9	11.9
Al ₂ O ₃	26.1	3.5	6.8	30.0	25.3	6.9
Fe ₂ O ₃	8.6	24.0	13.4	8.3	12.6	3.0
CaO	8.0	19.5	11.4	9.5	3.4	15.2
MgO	1.7	3.5	7.6	4.0	1.5	2.2
SO ₃	4.8	22.5	12.9	3.6	2.5	31.5
Alkali	0.0	1.5	1.3	0.2	1.8	22.0
Not Determined	2.9	0.0	0.4	2.6	0.0	7.3

TABLE II COMPARISON OF ESTIMATED AND OBSERVED PERFORMANCE OF EUROPEAN BROWN COALS

Coal	Performance	stagnating	fouling	Matt & Ferreday		Prediction		Slagging	f _s	Fouling	f _f	Fouling
				Critical Viscosity	B/A	Stagnating	R _s					
Ungarn	considerable	medium	medium	1395	0.247	low	1.088	medium	0.384	none	1.000	0.0
Leipzig	strong	medium	medium	904	1.621	high-severe	4.539	very high	0.106	strong	0.863	low
Niederlausitz	strong	medium	low	1268	0.611	medium	0.734	medium	0.456	medium	0.300	medium
Oberlausitz	none	none	none	1312	0.304	low	0.061	little	0.963	none	0.998	low
Nordbohmen	very strong	low	low	1440	0.224	low	0.246	little	0.086	very strong	0.627	medium
Salzkohle	strong	very strong	very strong	963	1.085	high-severe	3.038	very high	0.189	strong	0.091	very strong
												22.0
												1.8
												1.3
												1.5
												0.2
												1.8
												0.0
												0.0

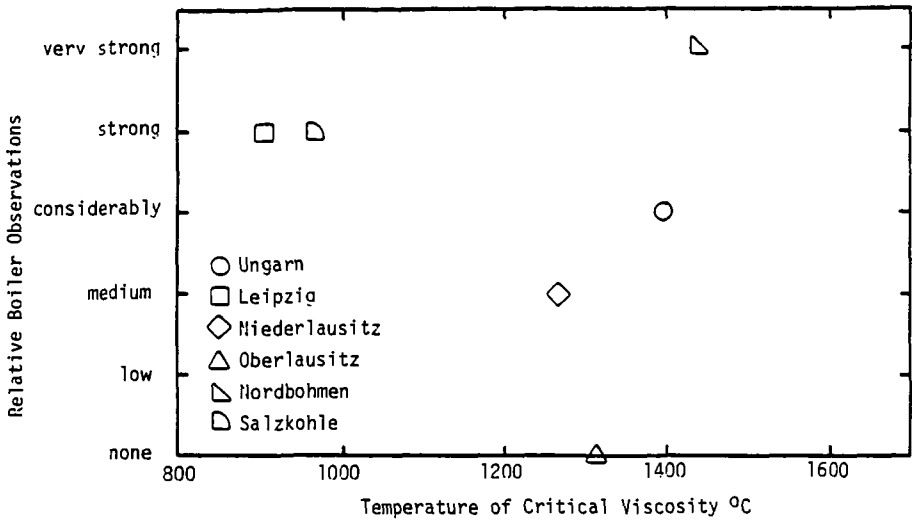


Figure 1a. Comparison of observed and predicted (T_{cv}) slagging performance of brown coal.

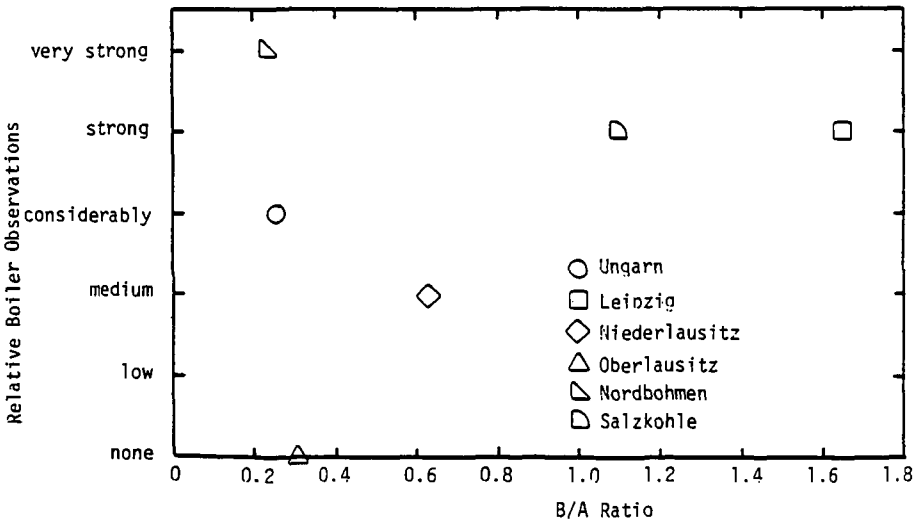


Figure 1b. Comparison of observed and predicted (B/A) slagging performance of brown coal.

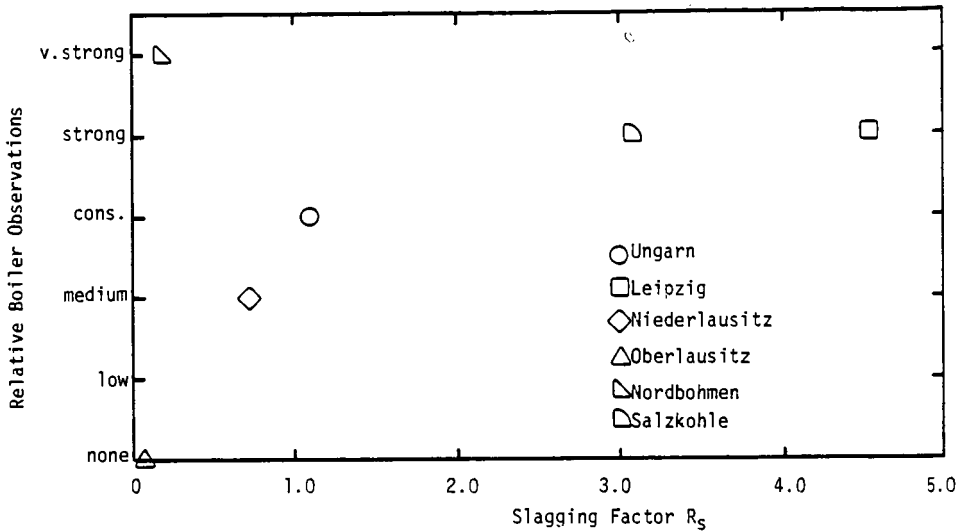


Figure 2a. Comparison of observed and predicted (R_S) slagging performance of brown coal.

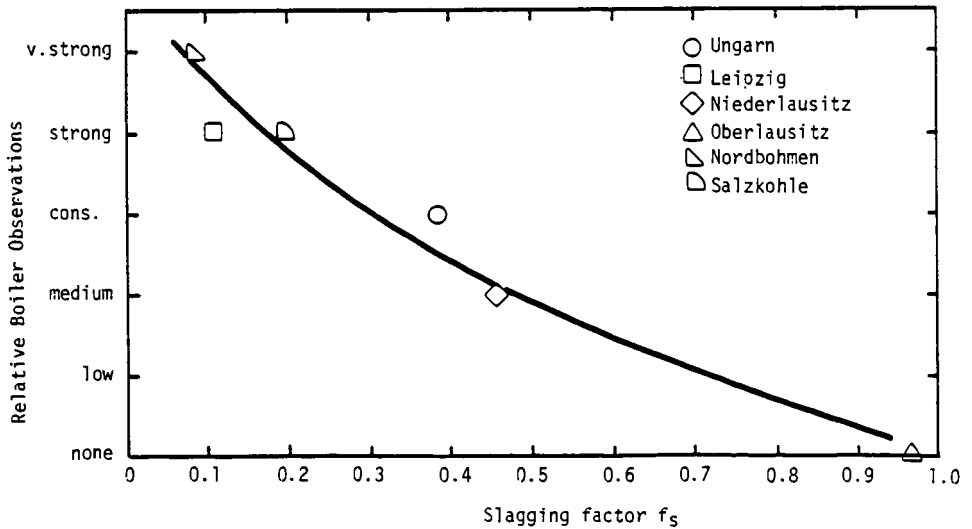


Figure 2b. Comparison of observed and predicted (f_S) slagging performance of brown coal.

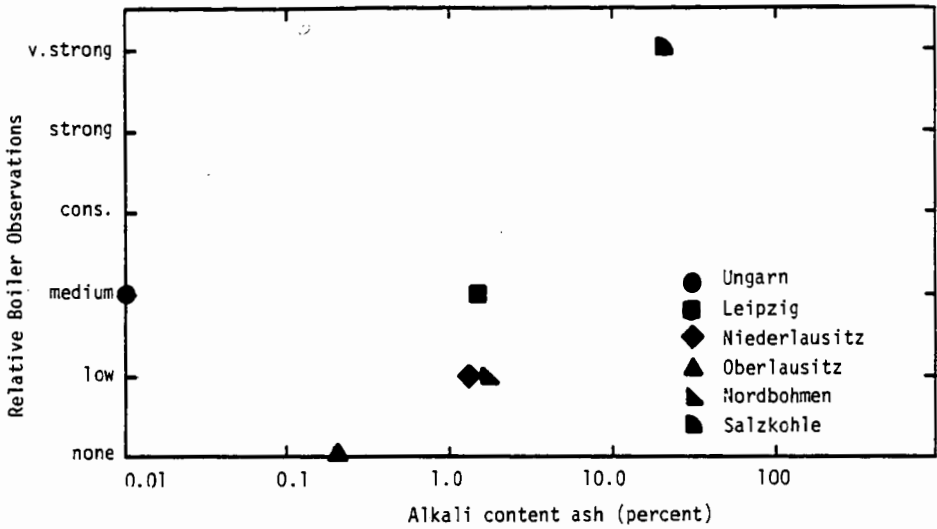


Figure 3a. Comparison of observed and predicted (Alkali content) fouling performance of brown coal.

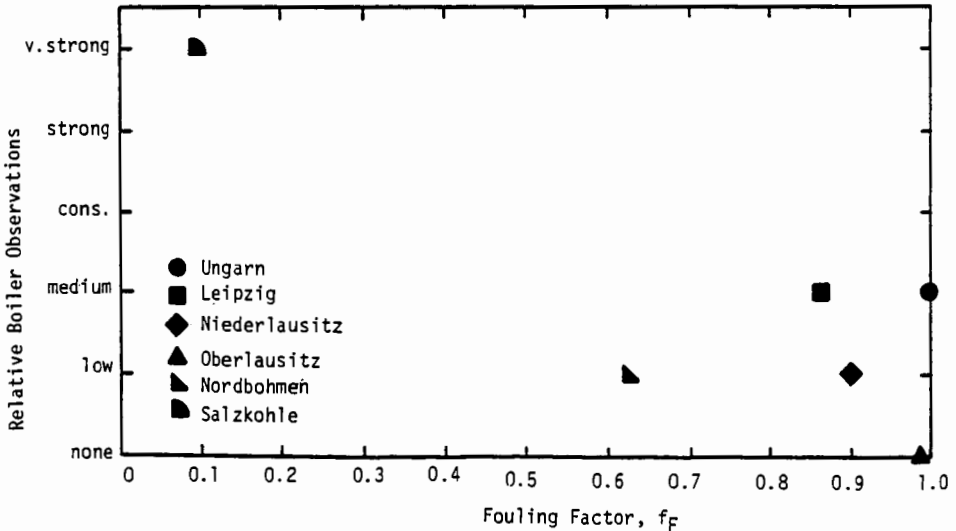


Figure 3b. Comparison of observed and predicted (f_F) fouling performance of brown coal.

References

- (1) Winegarteer, E. C., "Coal Fouling and Slagging Parameters," Book No. H-86 ASME, 1974.
- (2) Bryers, R. W., "On-Line Measurements of Fouling and Slagging (Full-Scale and Pilot Units) and Correlation with Predictive Indices in Conventionally Fired Steam Generators." Proceedings of the Low Rank Coal Technology Development Workshop, San Antonio, Texas, June, 1981.
- (3) Barrett, R. E., J. M. Murin, and G. A. Mack, and J. P. Dimmer, "Evaluating Slagging and Fouling Parameters," presented at the American Flame Research Committee Fall Meeting, Akron, Ohio, October, 1983.
- (4) Pollmann, S. and W. Albrecht, "Investigations of the Slagging Behavior of Bituminous Coals in Large Dry-Bottom Steam Generators," p. 85., in R. W. Bryers, "Fouling and Slagging Resulting from Impurities in Combustion Gases," Engineering Foundation, New York, 1983.
- (5) Altmann, W. "Beurteilung der Verschlackungs - und Verschmutzungsneigung fester Brennstoffe." XIV Kraftwerkstechnischen Kolloquium, Dresden, German Democratic Republic, October, 1982.
- (6) Pohl, J. H., "Errors in Predicting the Slagging and Fouling Behavior of Coals Based on Standard Techniques", XIV Kraftwerkstechnischen Kolloquium, Dresden, German Democratic Republic, October, 1982.
- (7) Blackmore, G., "Quality Coal for Electric Utility Use," Ninth Annual International Conference on Coal Gasification, Liquidification, and Conversion to Electricity," Pittsburgh, PA, August 1982.
- (8) Bryers, R. W., Private Communication, Foster Wheeler Development Corporation, 1984.
- (9) Richter, W., Private Communication, Energy and Environmental Research Corporation, 1984.
- (10) Watt, J. D. and F. Fereday, "The Flow Properties of Slags formed from the Ashes of British Coals: Part 1: Viscosity of Homogeneous Liquid Slags in Relation to Slag Composition." J. Inst. Fuel, v. 42, p.99, 1969.
- (11) Attig, R. C., and A. F. Duzy, "Coal Ash Deposition Studies and Applications to Boiler Design, Proceedings of the American Power Conference", v. 31, p. 299, 1969.

AN OVERVIEW OF MINERAL MATTER CATALYSIS OF COAL CONVERSION*

Thomas D. Padrick
Sandia National Laboratories, Albuquerque, NM 87185

INTRODUCTION

Since the 1920's, several studies have focused on the catalytic effects of inherent mineral matter on coal conversion.¹ In recent years, we have witnessed an increase in the level of coal research and the development of new coal utilization processes. In parallel with this activity, there have been reports on the effects of coal minerals on coal liquefaction, coal gasification, in-situ coal gasification, and other areas of coal utilization.²⁻⁵ This overview will deal primarily with recent results of mineral matter effects in coal liquefaction and coal gasification. The terms minerals, mineral matter, and ash will be used synonymously. An attempt will not be made to review the effects of all classes of minerals, but will only consider those minerals which have shown a large effect on coal conversion processes. A good review of the specific minerals present in a variety of coals can be found in the work of Gluskoter et al.⁶

COAL LIQUEFACTION

The Germans used coal liquefaction on a commercial scale from 1930 to the end of the second World War. They found that a catalyst could enhance liquid yields and help remove heteroatoms. The Bergius process used an iron oxide-aluminum catalyst at a 2-3% by coal weight concentration.

In recent years, it has been realized that mineral matter plays an important role in coal liquefaction,^{7,8,9} similar to the role of the added catalyst in the Bergius process. Several experimental techniques have been used to study the effects of minerals on coal liquefaction and to identify the specific catalytic phase.¹⁰ Most studies^{11,12} strongly imply that the iron sulfides are the most active species, and the other minerals appear to have little effect on enhancement of liquid yield or quality.

The specific role of pyrite (FeS_2) as a catalyst has been under investigation since pyrite was identified as the most active inherent mineral for coal liquefaction. Under liquefaction conditions, FeS_2 is transformed into a nonstoichiometric iron sulfide, Fe_{1-x}S ($0 < x < 0.125$). Thomas et al.¹³ studied the kinetics of this decomposition under coal liquefaction conditions, and concluded that the catalytic activity of FeS_2 is associated with radical initiation resulting from the pyrite-pyrrhotite transformation.

Several studies have investigated the possibility that defects in the pyrrhotite structure provide the sites for catalyst activity. A recent study¹⁴ found a linear correlation between the conversion to benzene or THF solubles and the atomic percent iron in

* This work supported by the U. S. Dept. of Energy at Sandia National Laboratories under contract no. DE-AC04-76DP00789.

the liquefaction residues. Montano *et al.*¹⁵ used *in situ* Mössbauer spectroscopy to study transformation of FeS_2 to Fe_{1-x}S . They observed a large pyrrhotite surface area at the reaction temperature (above 350°C).

Stohl and Granoff¹⁶ investigated the effects of pyrite particle sizes, pyrite defects and surface areas on coal liquefaction. They observed no effect due to surface area and concluded that the observed particle size effect was due to diffusional limitations in the transformation of pyrite to pyrrhotite.

While many studies indicate that pyrrhotites are probably involved in the liquefaction process, the exact mechanism by which pyrrhotite catalyzes the conversion of coal to oil is not clear. Based on the works of Thomas *et al.*¹³ and Derbyshire *et al.*,¹¹ one can suggest that a possible role of pyrrhotite is as a hydrogenation catalyst. However, more work is necessary on the surface properties of the pyrrhotites and the interaction with model compounds before a definite catalytic mechanism can be proposed.

COAL GASIFICATION

The gasification of coal involves two distinct stages: (1) devolatilization and (2) char gasification. Devolatilization occurs quite rapidly as the coal is heated above 400°C. During this period, the coal structure is altered, producing a less reactive solid (char), tars, condensable liquids and light gases. Nominally 40% of the coal is volatilized during this period. The less reactive char then gasifies at a much slower rate. We will discuss the effects of coal minerals on both devolatilization and char gasification.

A large volume of work has been reported on rapid devolatilization of coal (heating rates approximating process conditions).^{17,18} Recently, the effects of coal minerals on the rapid pyrolysis of a bituminous coal were reported by Franklin, *et al.*¹⁹ They found that only the calcium minerals affected the pyrolysis products. Addition of CaCO_3 reduced the tar, hydrocarbon gas and liquid yields by 20-30%. The calcium minerals also altered the oxygen release mechanism from the coal. Franklin, *et al.* attribute these effects to CaCO_3 reduction to CaO , which acts as a solid base catalyst for a keto-enol isomerization reaction that produces the observed CO and H_2O .

Walker and co-workers at the Pennsylvania State University have investigated the reactivity of a variety of coals during gasification in air, CO_2 , H_2 and steam.²⁰⁻²³ Hippo and Walker²¹ found a linear correlation between reactivity and CaO content in the ash. They also observed an increase in reactivity with MgO , up to about 1%. They found no correlation between reactivity and iron content or total K or Na content. In their studies on hydrogen and steam gasification, the Penn State group used coals demineralized by acid washing to study mineral matter effects. While changes were observed in these studies, it was difficult to attribute these changes to catalytic effects or physical effects.

Mahajan *et al.*²⁴ observed that the presence of pyrite in coal had a beneficial catalytic effect on hydrogenation at 570°C. They suggested that the catalytic activity was due to pyrrhotite formation. Hüttinger and Krauss²⁵ reached a similar conclusion concerning the catalytic activity of pyrite, and concluded that

above 850°C, iron enhanced the methane formation if the H₂ pressure was sufficiently high.

Padrick *et al.*²⁶ observed enhancement of the hydrogasification rate of a Pittsburgh Seam coal at 1000°C when various iron-containing minerals were mixed with the coal. They investigated the chemical effect of the minerals by measuring H₂/D₂ exchange rates, and also determined the physical effect of the mineral addition on the resultant surface areas and pore volumes of the chars. While the correlation of 1000°C hydrogasification rates with measured parameters was somewhat better including the chemical effects of the minerals, it was concluded that the gasification rates for the various sources of reduced iron were primarily due to the physical interaction of the minerals with the coal.

REFERENCES

1. Marson, C. B. and Cobb, J. W., *Gas J.* 171, 39 (1925).
2. Davidson, R. M., "Mineral Effects in Coal Conversion," Rept. No. ICTIS/TR22, IEA Coal Research, London, January 1983.
3. Otto, K., Bortosiewicz, L., and Shelef, M., *Fuel* 58, 85 (1979).
4. Fisher, J., Young, J. E., Johnson, J. E., and Jonke, A. A., Report ANL 77-7 (1977).
5. Plogman, H. and Kuhn, L., Proceedings of the International Conference on Coal Science, Düsseldorf, Germany, September 7-9 (1981).
6. Gluskoter, H. J., Shimp, N. F. and Ruch, R. R., in "Chemistry of Coal Utilization. 2nd Supplementary Volume," John Wiley and Sons, New York, NY, pp. 369-424 (1981).
7. Granoff, B. and Traeger, R. K., *Coal Process. Technol.* 15, (1979).
8. Mukherjee, D. K. and Chowdhury, P. A., *Fuel* 55, 4 (1976).
9. Gray, David, *Fuel* 57, 213 (1978).
10. Gray, J. and Shah, Y. T. in "Reaction Engineering in Direct Liquefaction," Adison Wesley Pub. Co., New York, NY (1981).
11. Derbyshire, F. J., Varghese, P. and Whitehurst, D. D., Preprints, Amer. Chem. Soc., Div. Fuel Chem. 26, No. 1, 84 (1981).
12. Whitehurst, D. D., Mitchell, F. U. and Farcasiu, M., in "Coal Liquefaction. The Chemistry and Technology of Thermal Processes," Academic Press, New York, NY, pp. 163-177 (1980).
13. Thomas, M. G., Padrick, T. D., Stohl, F. V. and Stephens, H. P., *Fuel* 61, 761 (1982).
14. Montano, P. A. and Granoff, B., *Fuel* 59, 214 (1980).

15. Montano, P. A., Bommanavar, A. S., and Shah, V., Fuel 60, 703 (1981).
16. Stohl, F. V. and Granoff, B., 90th Annual Meeting of the AIChE, Houston, TX (1981).
17. Anthony, D. B. and Howard, J. B., AIChE J. 22, 625 (1976).
18. Stangby, P. C. and Sears, P. L., Fuel 60, 131 (1980).
19. Franklin, H. D., Peters, W. A. and Howard, J. B., Preprints, Amer. Chem. Soc., Div. Fuel Chem. 26, No. 2, 121 (1981).
20. Jenkins, R. G., Nandi, S. P. and Walker, P. L. Jr., Fuel 52, 288 (1973).
21. Hippo, E. J. and Walker, P. L. Jr., Fuel 54, 245 (1975).
22. Tomita, A., Mahajan, O. P. and Walker, P. L. Jr., Fuel 56, 137 (1977).
23. Linares-Solano, A., Mahajan, O. P. and Walker, P. L. Jr., Fuel 58, 327 (1979).
24. Mahajan, O. P., Tomita, A., Nelson, J. R. and Walker, P. L. Jr., Fuel 56, 33 (1977).
25. Hüttinger, K. J. and Krauss, W., Fuel 60, 93 (1981).
26. Padrick, T. D., Rice, J. K. and Massis, T. M., Preprints, Amer. Chem. Soc., Div. Fuel Chem. 27, No. 3, 300 (1982).